3.1 对流的分类

上节课回顾

（1）对流单体　　（2）多单体　　（3）超级对流单体

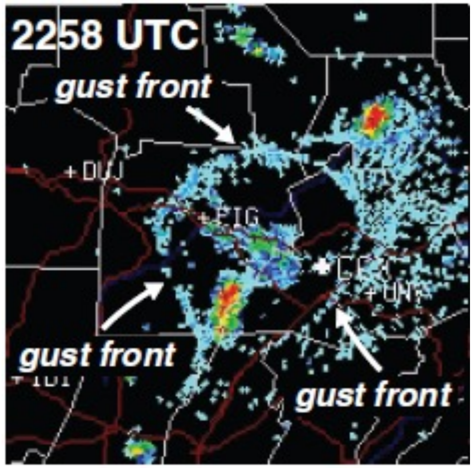

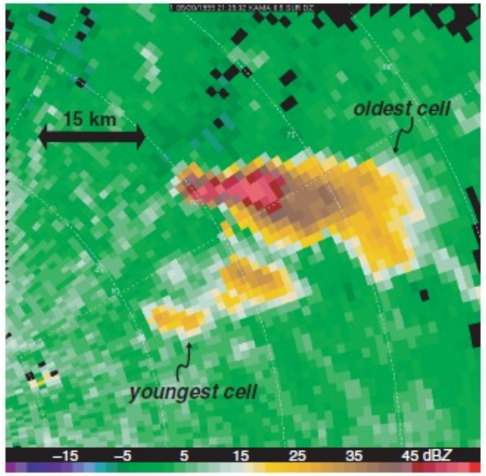

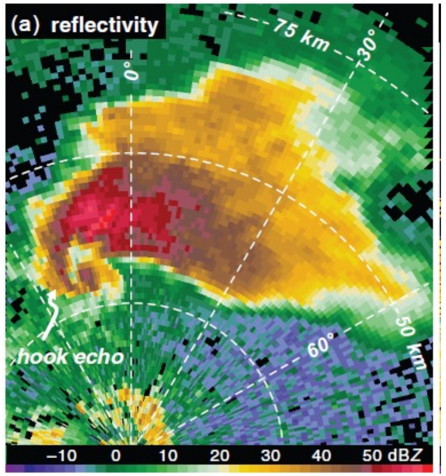

上节课回顾

（1）基本特征

1）只有一支上升气流，没有有组织的后继对流

2）生命期

$$\tau \approx \frac{H}{w_0} + \frac{H}{v_t}$$

H: surface – EL，~ 10 km

w_0: 平均上升速度，~ 5–10 m/s

v_t: 降水粒子的平均下降速度，~ 5 – 10 m/s

τ：~ 30 – 60 分钟

上节课回顾

3）生成环境

- 环境垂直风切变很弱，上升气流主要由浮力引起，没有明显的天气尺度强迫，比如锋面抬升、温度和湿度平流等。
- 主要由边界层日变化引起，往往午后发展。
- CAPE：几百–2000 J/kg.
- w: 5–40 m/s

4）天气

偶尔有冰雹、Gust wind，持续时间很短。

5）移动：随环境风（0–6km 平均风）移动

3.2 对流单体（对流系统的基本单元）

上节课回顾

（2）生命史

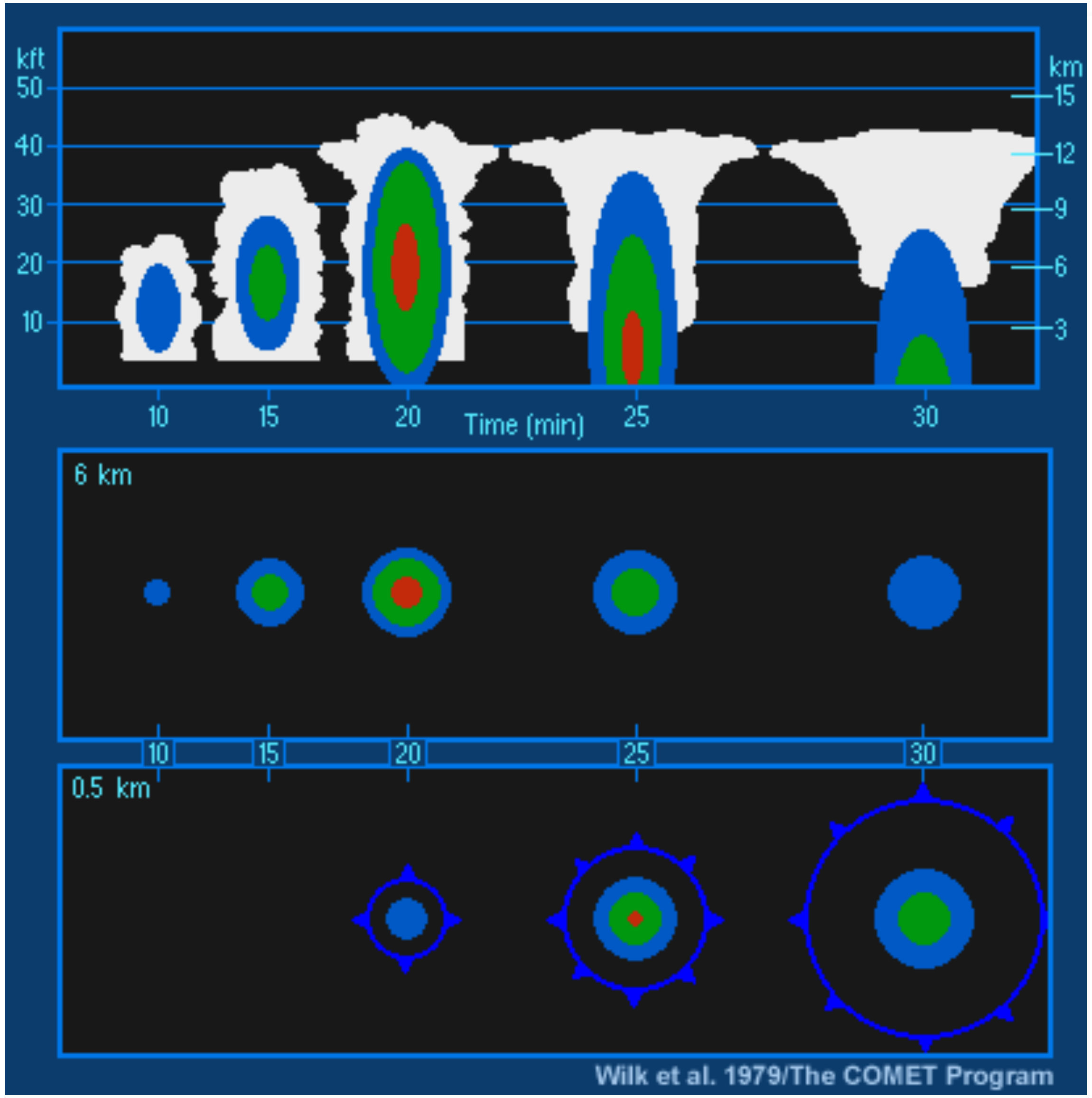

颜色代表雷达回波

（3）冷池触发对流的物理机制

上节课回顾

1） 涡度倾向方程

由中尺度方程组，Boussinesq近似（$\nabla \cdot \vec{v} = 0$）

针对对流尺度，忽略摩擦和科氏力项

$\bar{\rho}$为常数

$$
\begin{cases}
\dfrac{du}{dt} = -\dfrac{1}{\bar{\rho}}\dfrac{\partial p'}{\partial x} \\
\dfrac{dv}{dt} = -\dfrac{1}{\bar{\rho}}\dfrac{\partial p'}{\partial y} \\
\dfrac{dw}{dt} = -\dfrac{1}{\bar{\rho}}\dfrac{\partial p'}{\partial z} - \dfrac{\rho'}{\bar{\rho}}g = -\dfrac{1}{\bar{\rho}}\dfrac{\partial p'}{\partial z} + B
\end{cases}
$$

$$\frac{d\eta}{dt} = -\frac{\partial B}{\partial x}$$

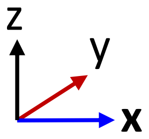

纸面向里为+，向外为-

上节课回顾

a. Updraft, 水汽凝结， B极大

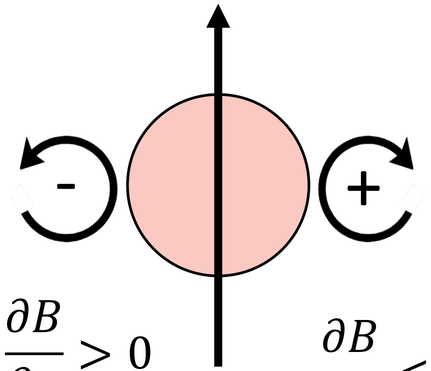

$\frac{\partial B}{\partial x} > 0$　　$\frac{\partial B}{\partial x} < 0$

η减小　　η增大

b. Downdraft, 水汽蒸发， B极小

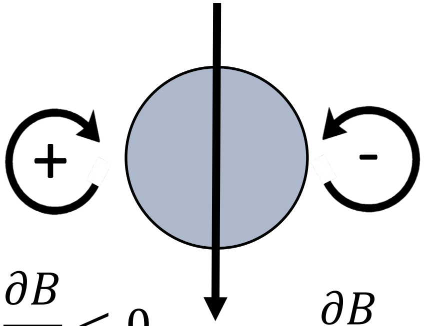

$\frac{\partial B}{\partial x} < 0$　　$\frac{\partial B}{\partial x} > 0$

η增大　　η减小

（1）基本特征

上节课回顾

1）尺度　可持续几个小时（1–3h)，水平范围可达到中β、中α尺度（100 – 400 km)

2）天气　强天气：闪电，强直线大风，可能会有大冰雹，短时强降水和龙卷。

3）系统的运动

- 单体沿着0-6km的平均风移动
- 风暴系统的传播（新单体的生成方向）一般位于阵风锋的下切变方向。

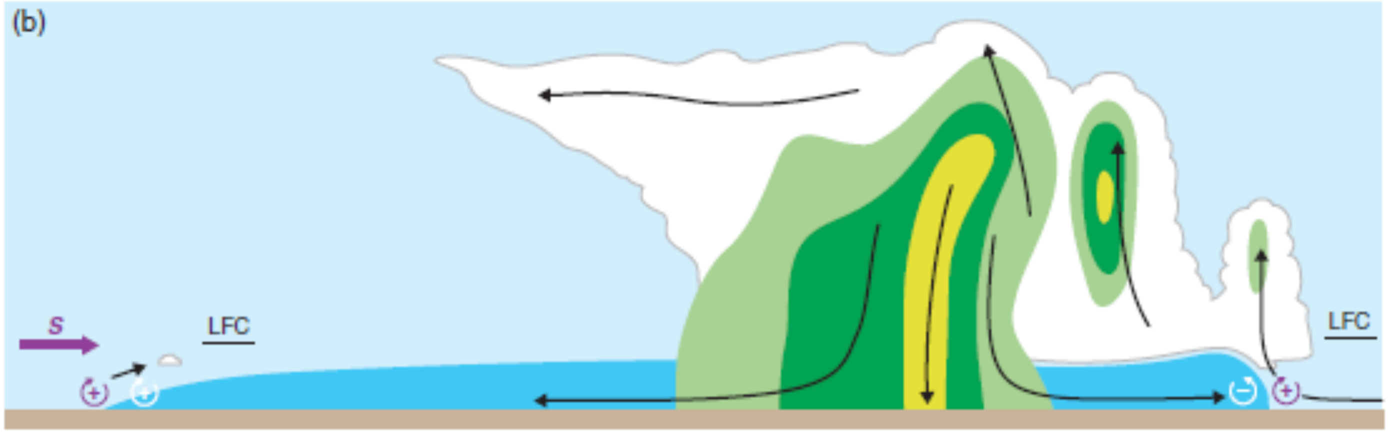

4）生命史

上节课回顾

- 对流单体成熟，形成冷池；
- 旧的单体不断消亡，新的单体不断生成；
- 多个单体的冷池叠加，强度越来越强，最终切断暖湿气流，导致雷暴消亡。

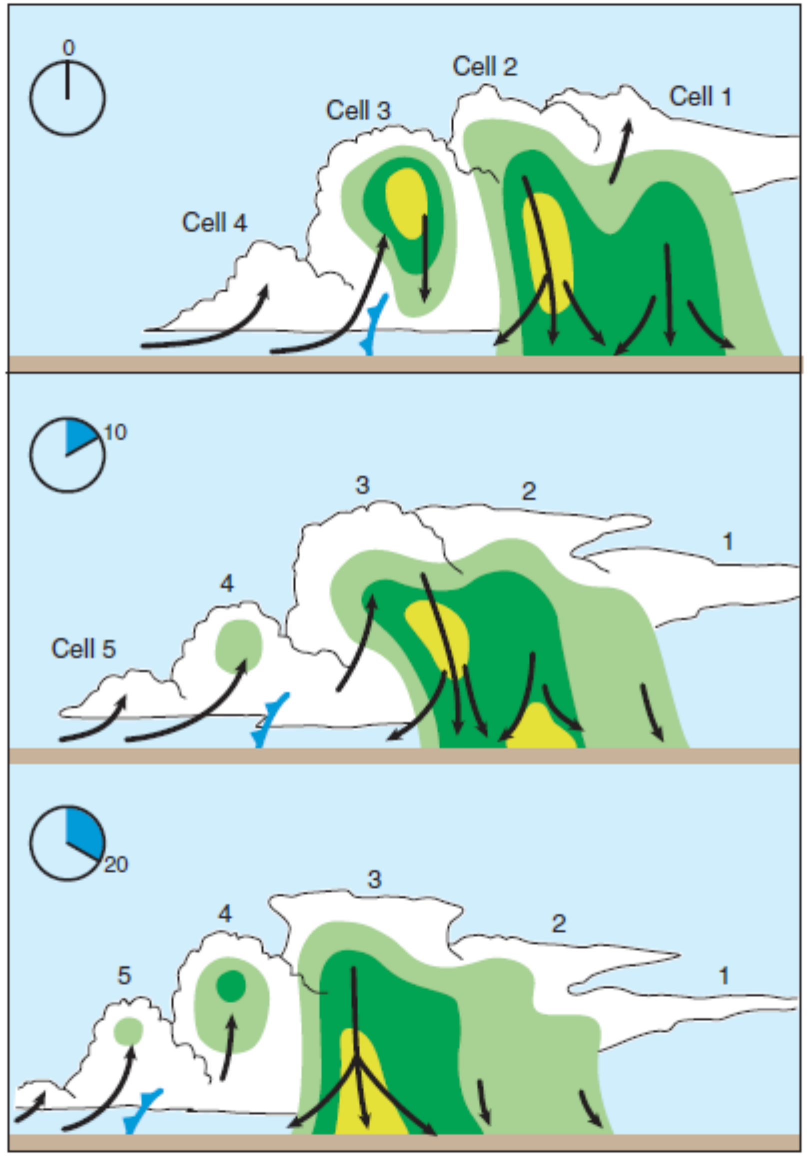

Figure 8.11 Schematic of the evolution of multicellular convection. Refer to the text for details. (Adapted from Doswell [1985].)

RKW理论

上节课回顾 当垂直风切变有足够大的水平涡度和冷池产生的水平浮力梯度造成的反向水平涡度平衡，气块得到最大的抬升，最可能达到LFC。

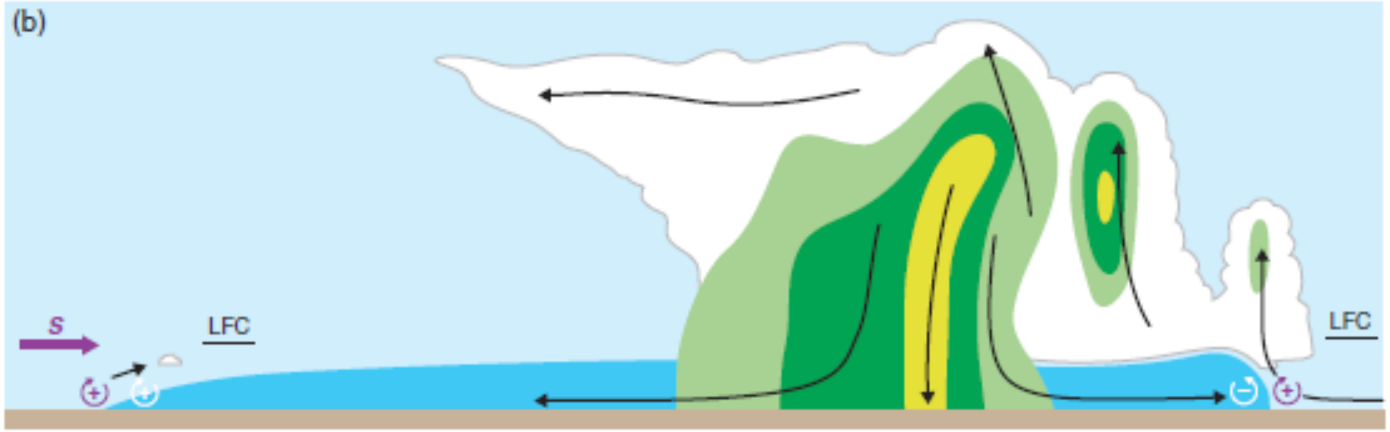

Figure 8.12 Comparison of lifting by the gust front in (a) a no-shear, single-cell environment and (b) a moderate-shear, multicell environment (the shear is westerly). Rain and hail are schematically indicated by the green and yellow shading. Evaporatively cooled outflow is shaded dark blue. Cloud is white. Some select storm-relative streamlines are shown as black arrows. The LFC is also indicated. The sense of the horizontal vorticity induced by the cold pools is indicated with white circular arrows. In (b), the sense of the horizontal vorticity associated with the environmental vertical wind shear is indicated with purple circular arrows. Moreover, the modification of the depth and slope of the leading portions of the cold pool by its interaction with the environmental shear, along with the effect on the nature of the lifting along the gust front, is also reflected in (b). Compare the depths of the western and eastern outflow heads in (b) to each other, as well as to those drawn in (a).

3.4 超级对流单体

定义：包含一个准稳态旋转上升气流，持续时间远长于单体对流，它是危险性对流风暴。

A single dominant updraft and associated mesocyclone

超级对流单体：2021.6.13 四川若尔盖

超级对流单体：2021.10.3 四川若尔盖

A supercell with a hail core near Stratford, Texas on May 18, 2023.

超级对流单体的其他例子

A schematic of supercell

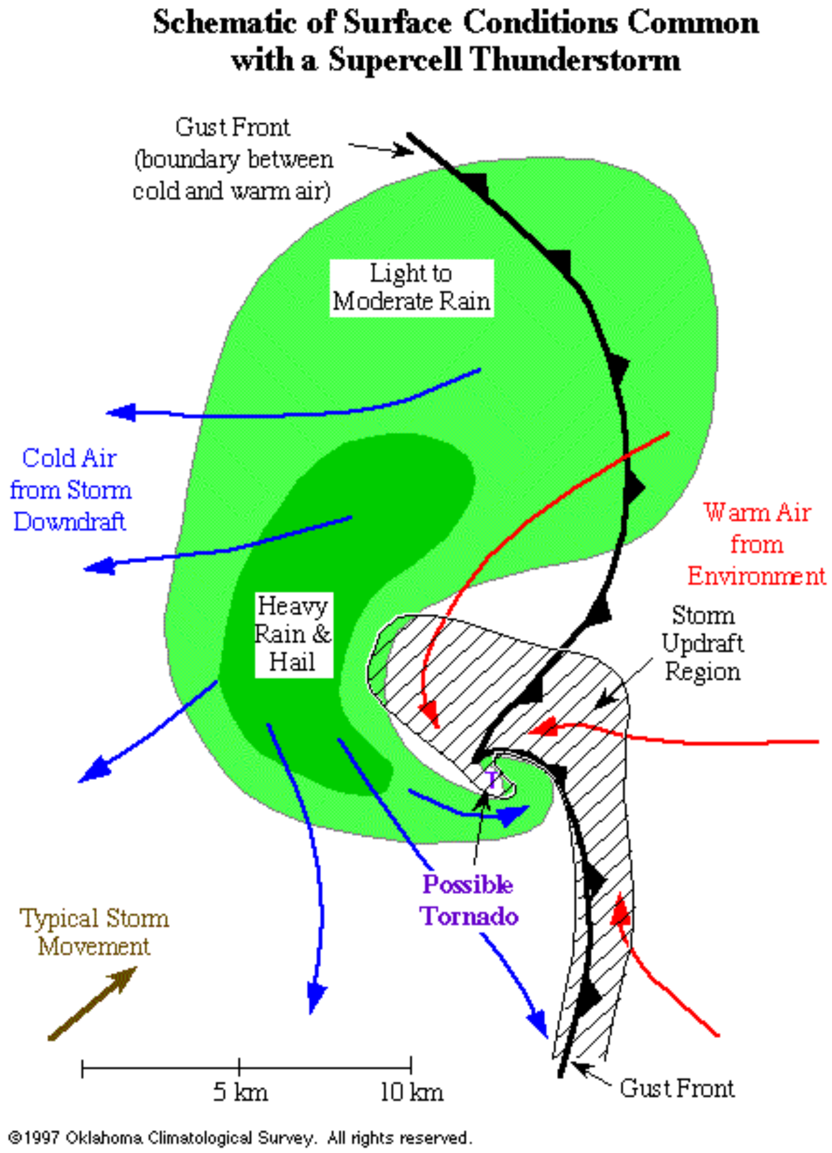

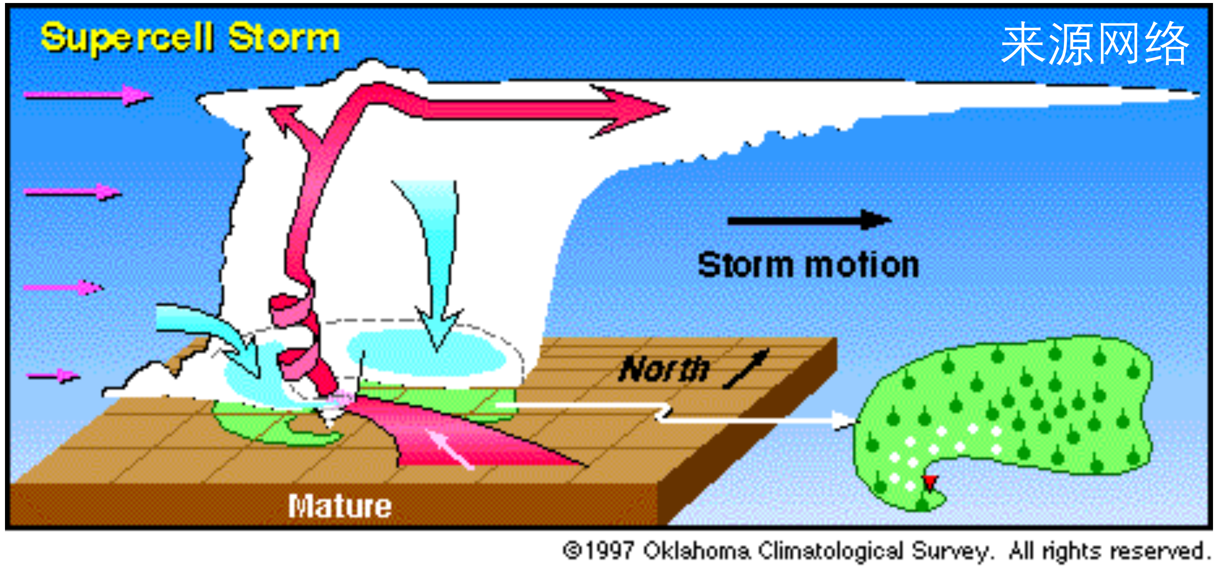

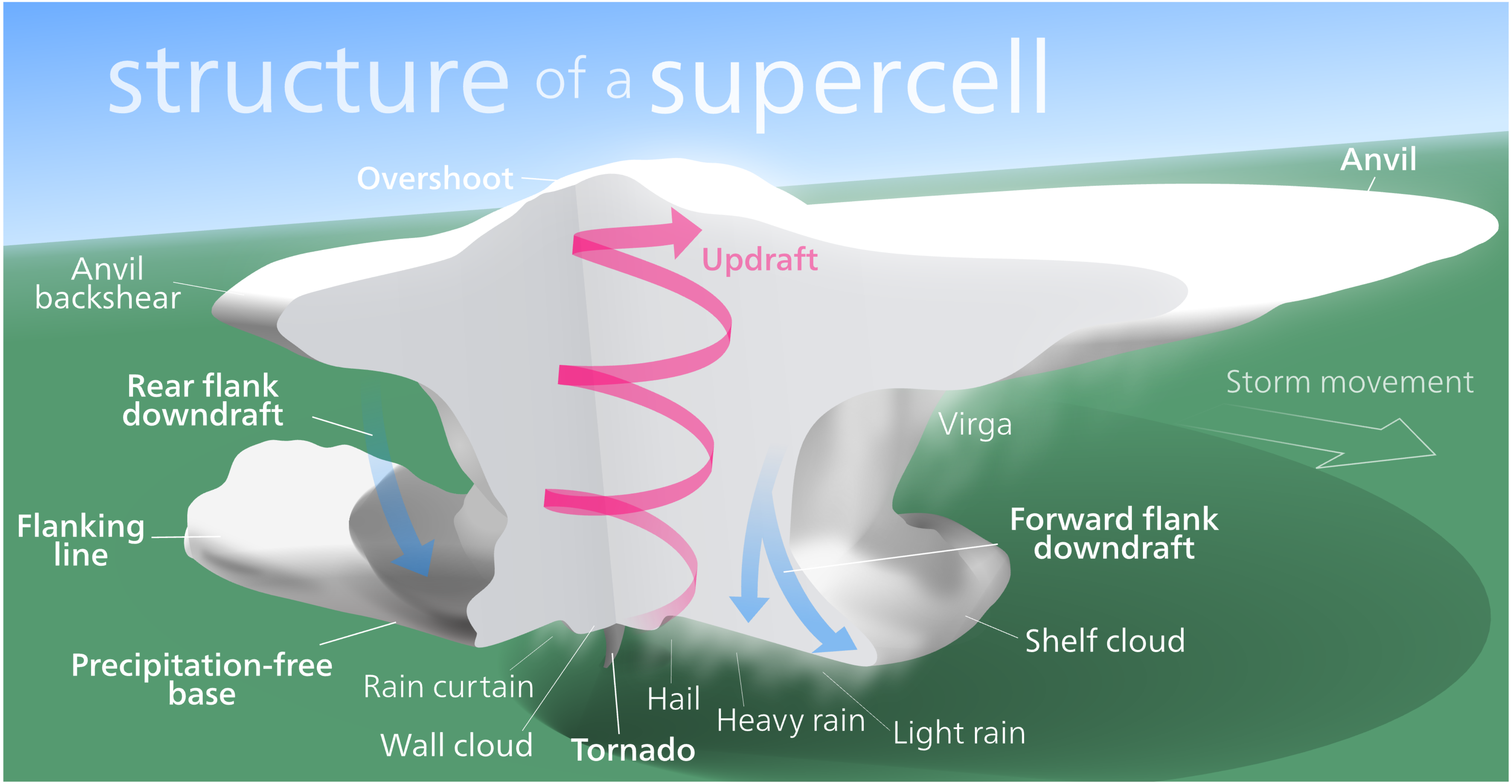
structure of a supercell
Overshoot
Anvil
Updraft
Anvil backshear
Rear flank downdraft
Storm movement
Virga
Flanking line
Forward flank downdraft
Shelf cloud
Precipitation-free base
Rain curtain
Hail
Heavy rain
Light rain
Wall cloud
Tornado

（1） 一般特征

1） 最少见，但灾害最重；

Hail (直径可大于5cm), 强龙卷基本上都是超级单体造成。

2） 生命期：1–4h，可达8h。

3） 上升气流中有一个持续性(>20分钟）深厚中气旋，直径3–8 km, 一般达到上升气流的一半高度，涡度为O(0.01) s^{-1}.

不同于阵风锋前的瞬变浅薄中涡旋。

4）生成环境： >20 m/s的0–6 km垂直风（long-curved hodograph），CAPE>1000 J/kg (不必要很大)

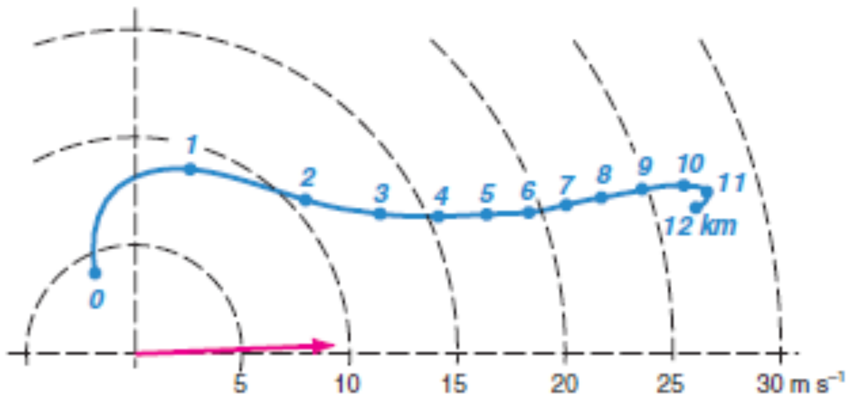

5） 上升气流的驱动：扰动气压垂直梯度力

6） 系统移动

- 明显偏离平均风
- 气旋性超级单体向平均切变矢量的右侧移动
- 反气旋性超级单体向平均切变矢量的左侧移动
- 分裂：两个分裂的单体对称移动，往往其中一个消亡，另一个发展加强。

(2) 超级单体结构

1） **Radar signature**

Hook echo: lower level reflectivity minimum

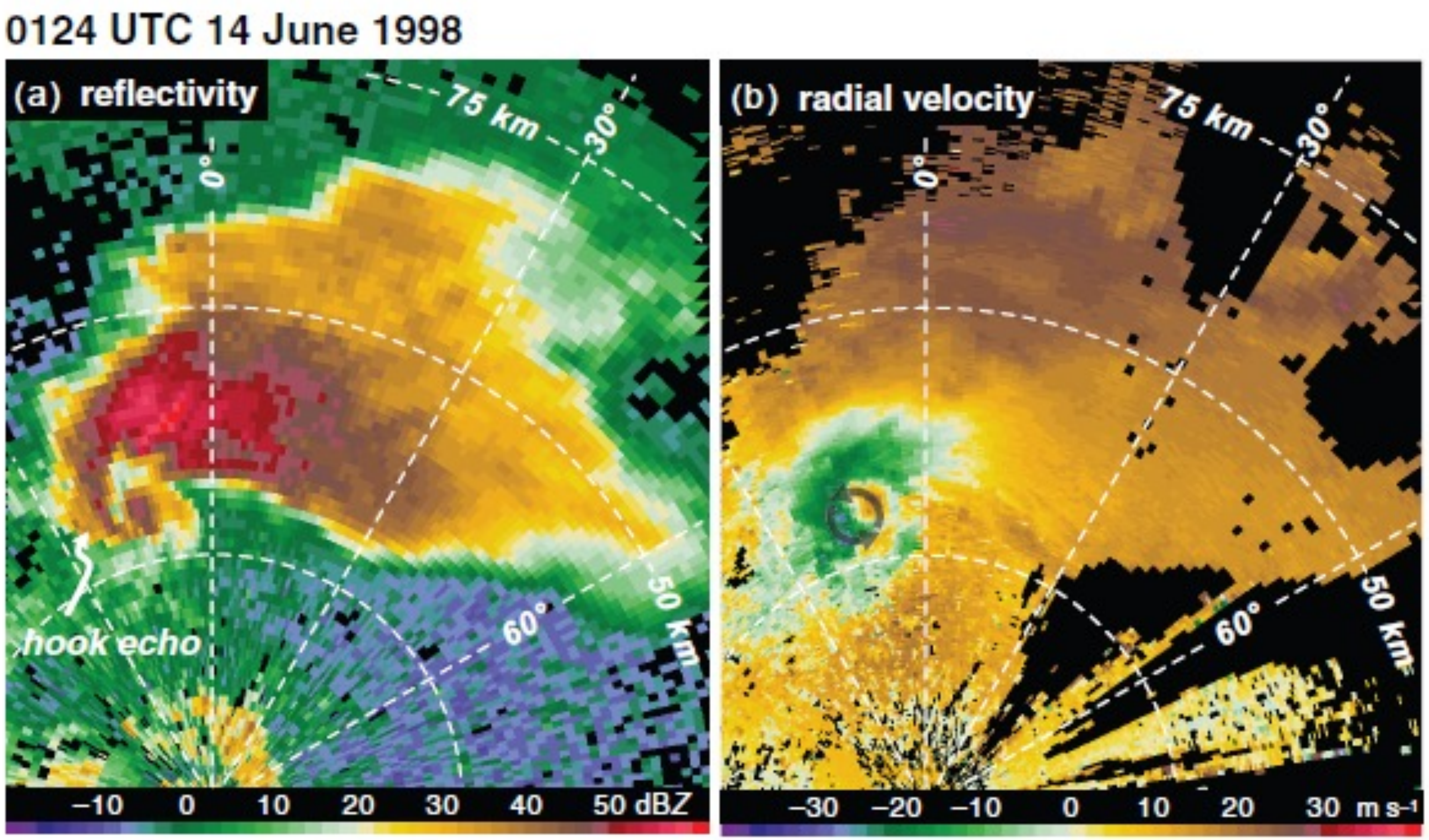

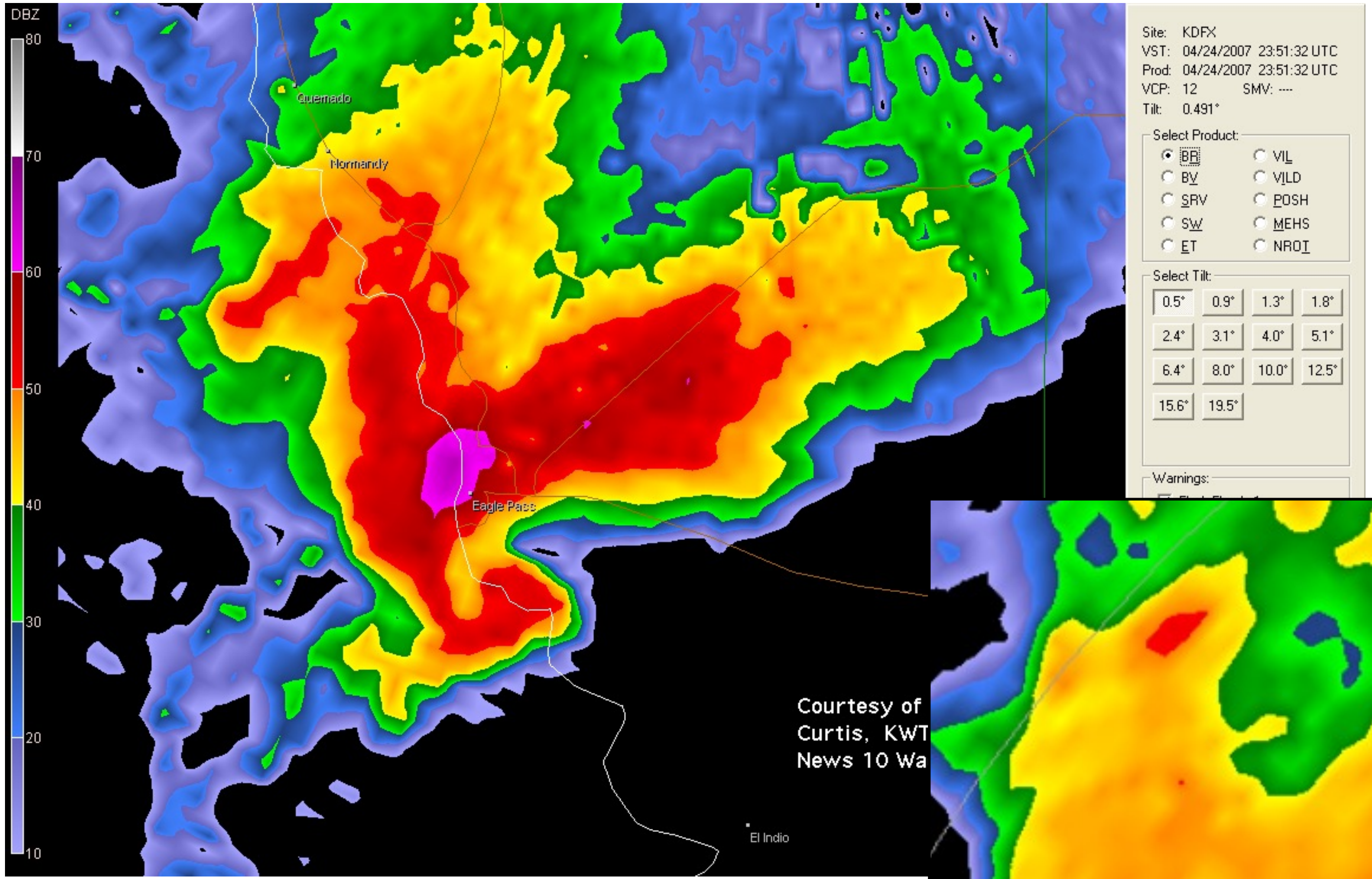

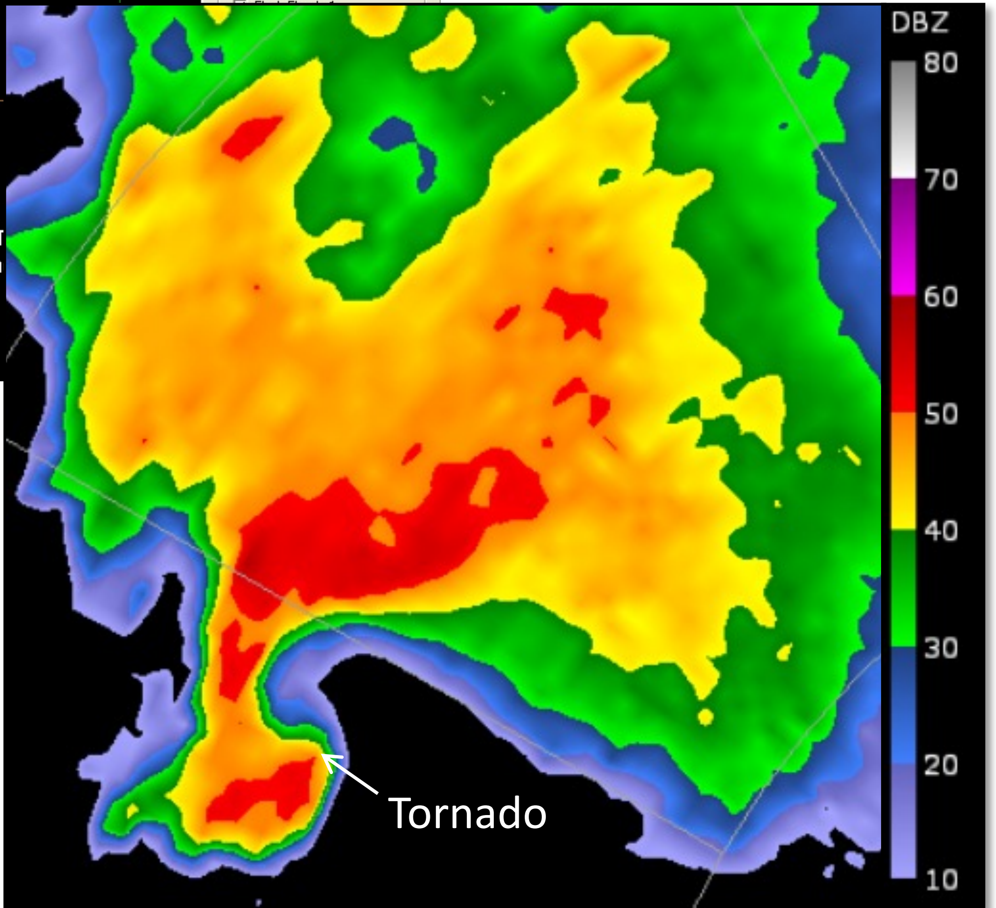

2016江苏盐城
阜宁 EF4 龙卷
母体超级单体

Bounded weak echo region (BWER)

WER at lower levels

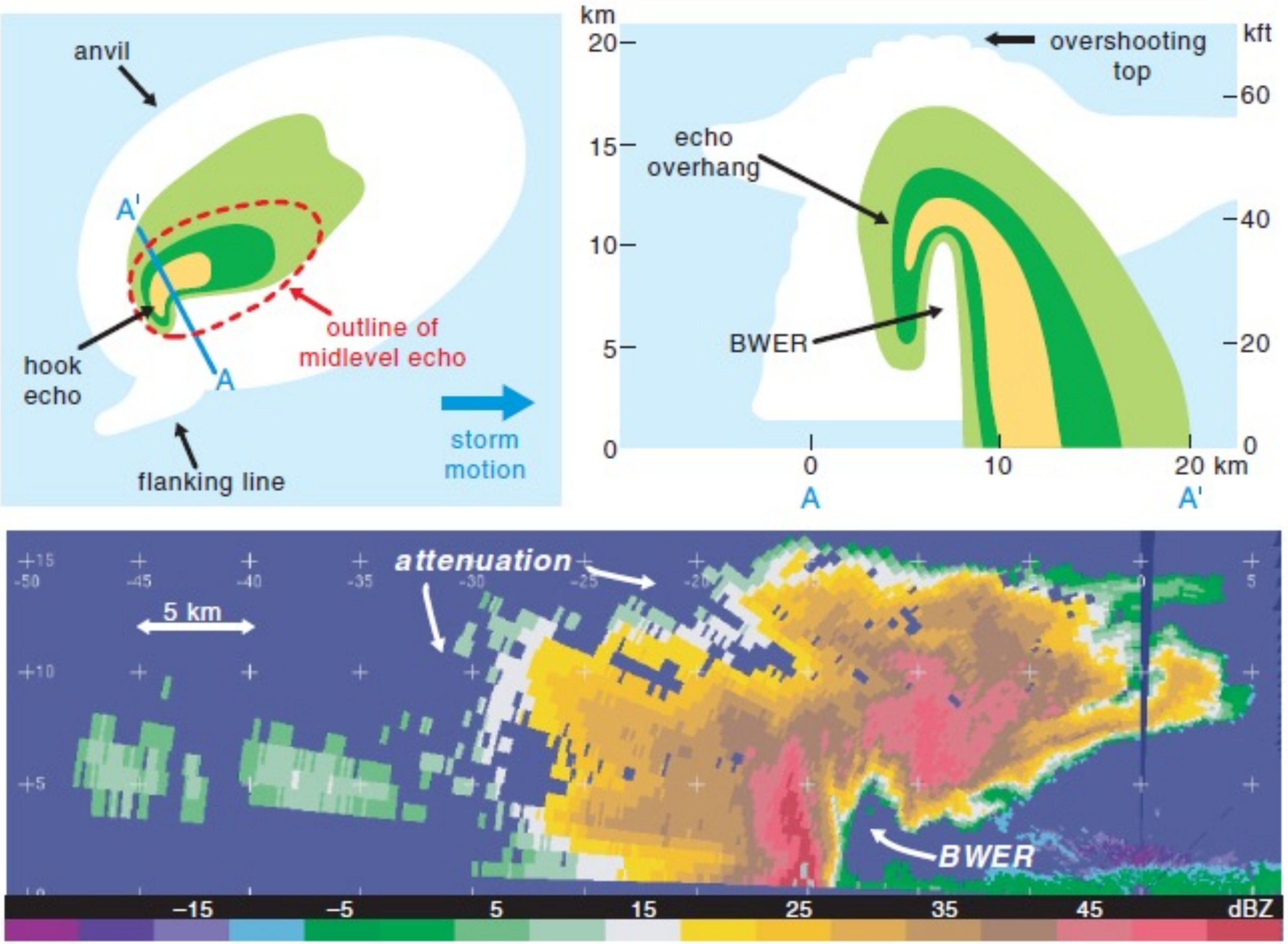

Bounded weak echo region (BWER)

WER at lower levels

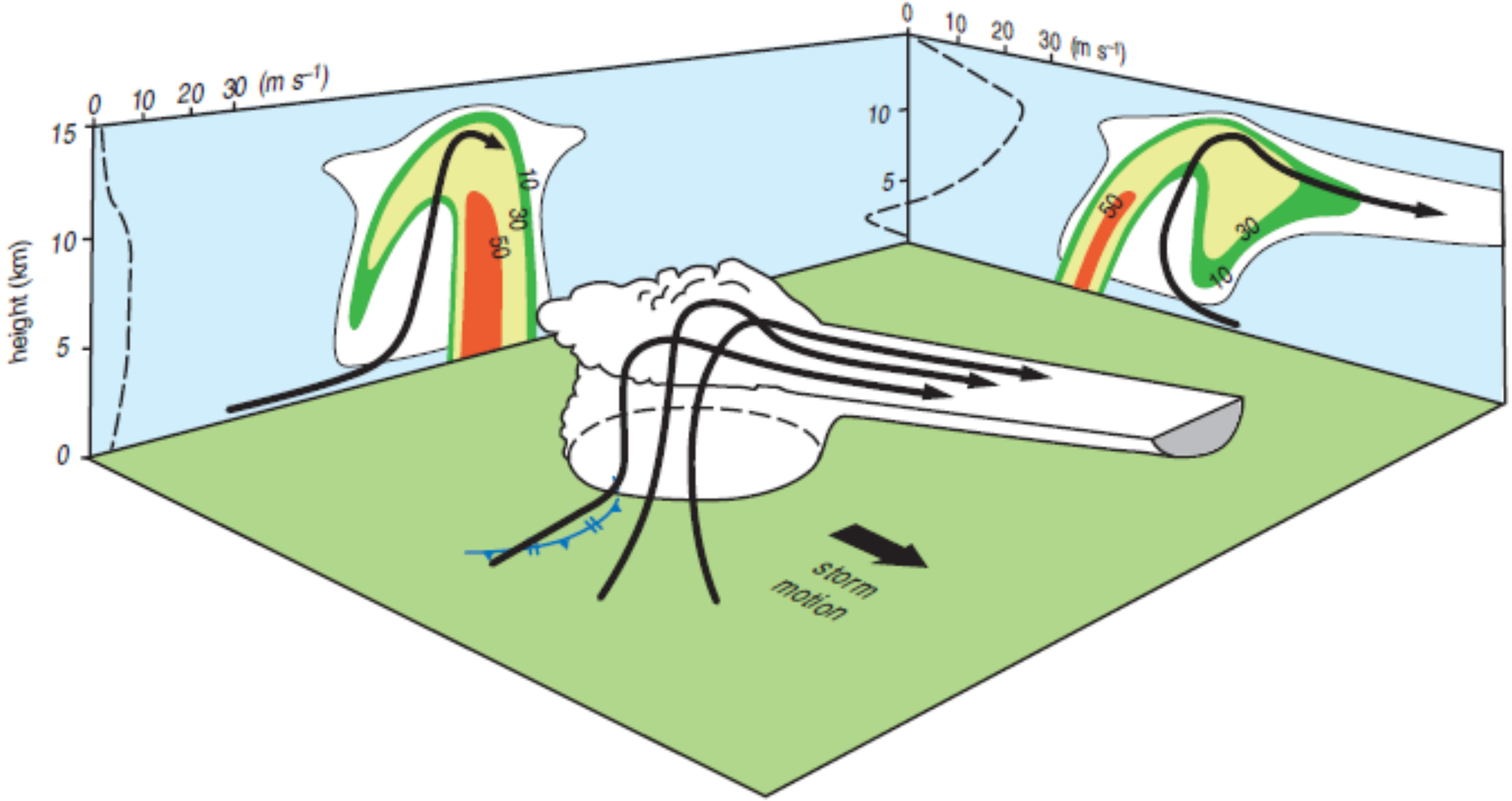

Figure 8.19 Perspective view of a supercell depicting storm-relative airflow and reflectivity structure. The reflectivity contours are 10, 30, and 50 dBZ. The rear-flank gust front also is shown. (Adapted from Chisholm and Renick [1972].)

2） Cloud features

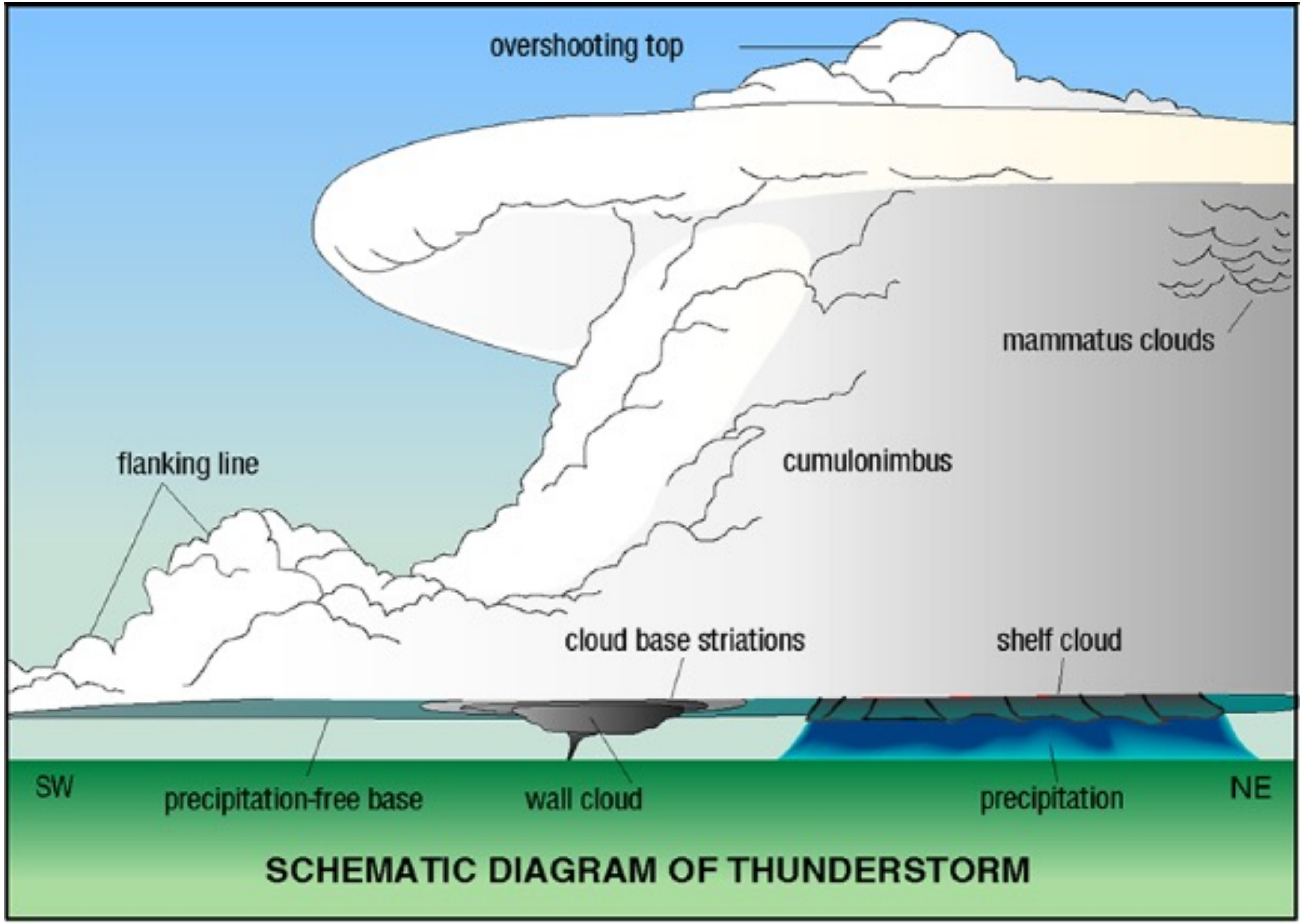

Wall cloud: 上升气流底部雨区潮湿冷空气卷入上升气流首先达到LCL。

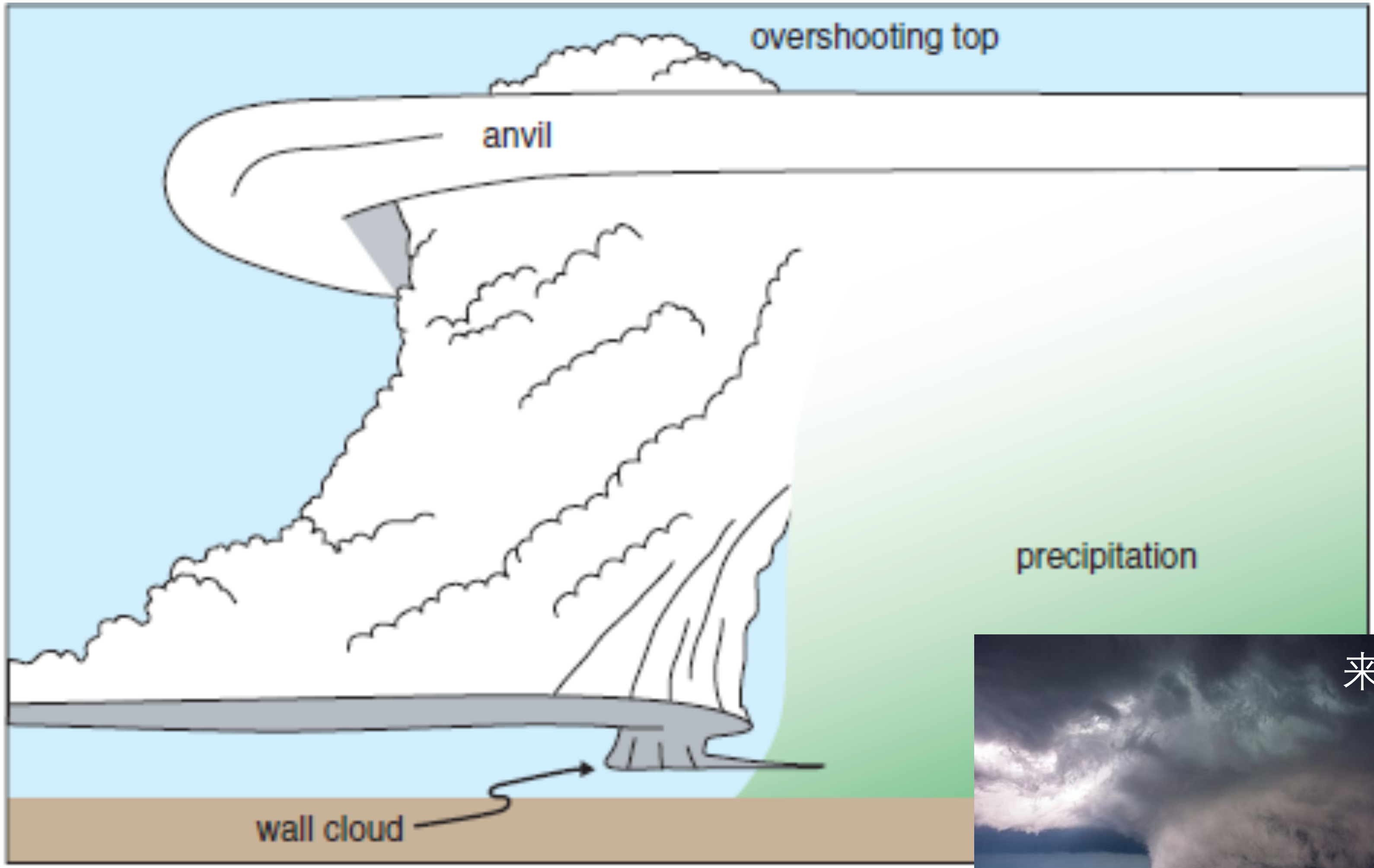

Wall cloud: 上升气流底部雨区潮湿冷空气卷入上升气流首先达到LCL。

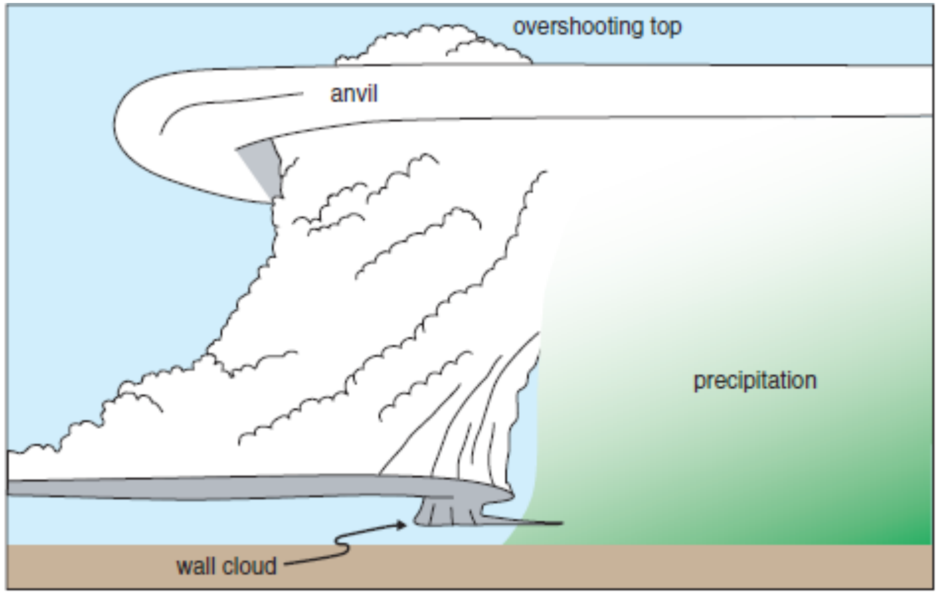

Wall cloud

来源网络

Wall cloud

来源网络

Wall cloud

来源网络

Overshooting cloud

来源网络

Overshooting cloud

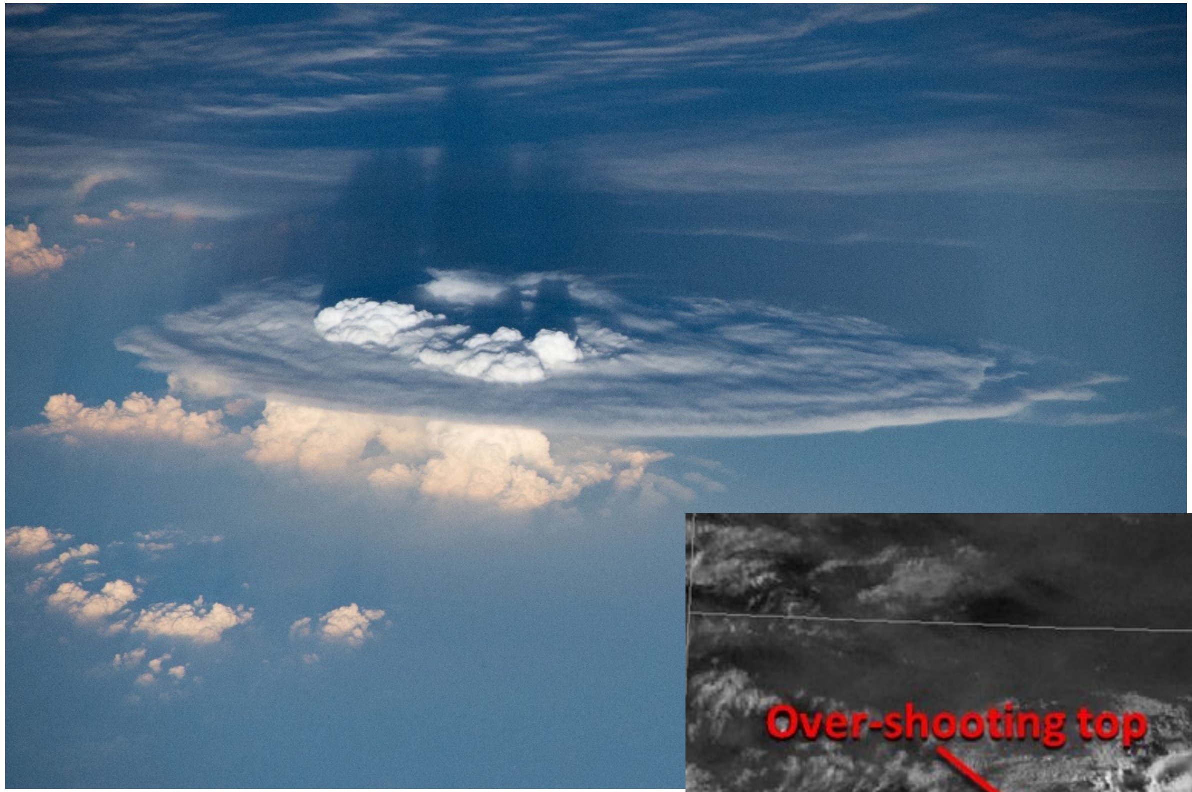

来源网络

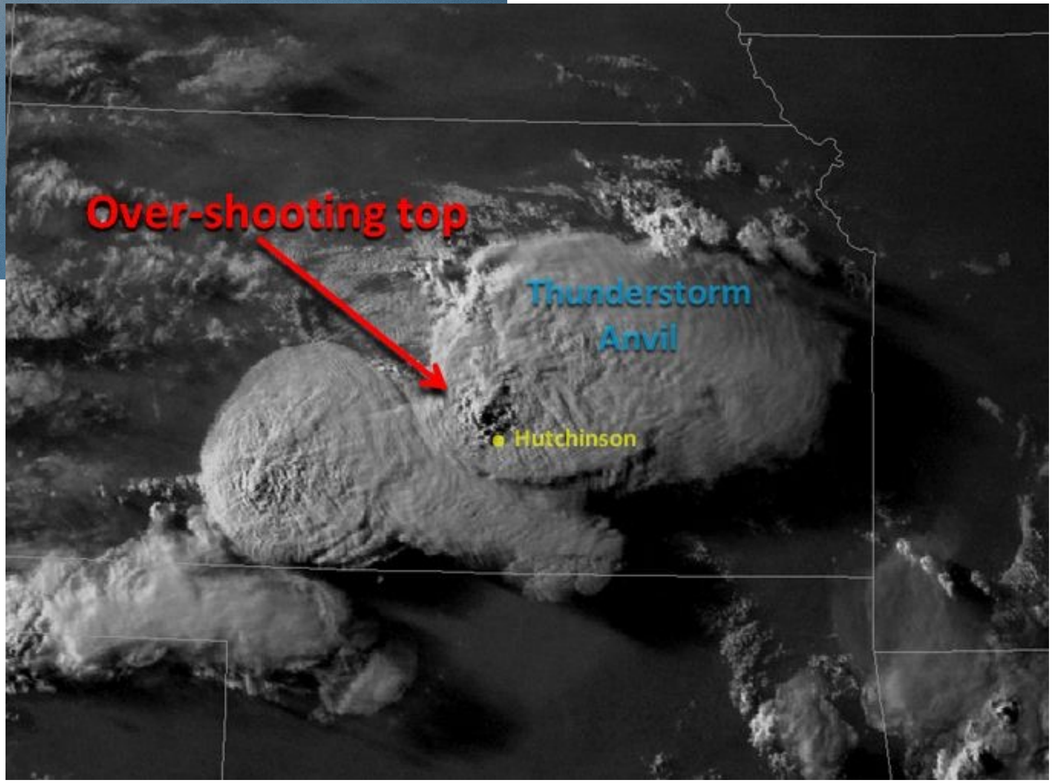

来源网络

Mammatus clouds

Hanging protuberances, like pouches, on the undersurface of a cloud.

来源网络

Mammatus clouds

摄影：刘屹靖

Mammatus clouds

摄影：刘屹靖

Mammatus clouds

2020.8.9 19.00 乌兰察布

摄影：刘屹靖

Mammatus clouds

2021.6.25 19.00 河北沽源县

摄影：刘屹靖

Shelf clouds

A low-level, horizontal, wedge-shaped arcus cloud associated with a convective storm's gust front (or occasionally a cold front).

The shelf cloud is attached to the convective storm's cloud base. Rising motion can be seen in the leading (outer) part of the shelf cloud, while the underside appears turbulent and tattered.

摄影： 刘屹靖

Shelf clouds

2020.8.1 18.35 呼伦贝尔

摄影：刘屹靖

3） Flanking line

Located at right-rear flank relative to storm motion

比主上升支浅薄

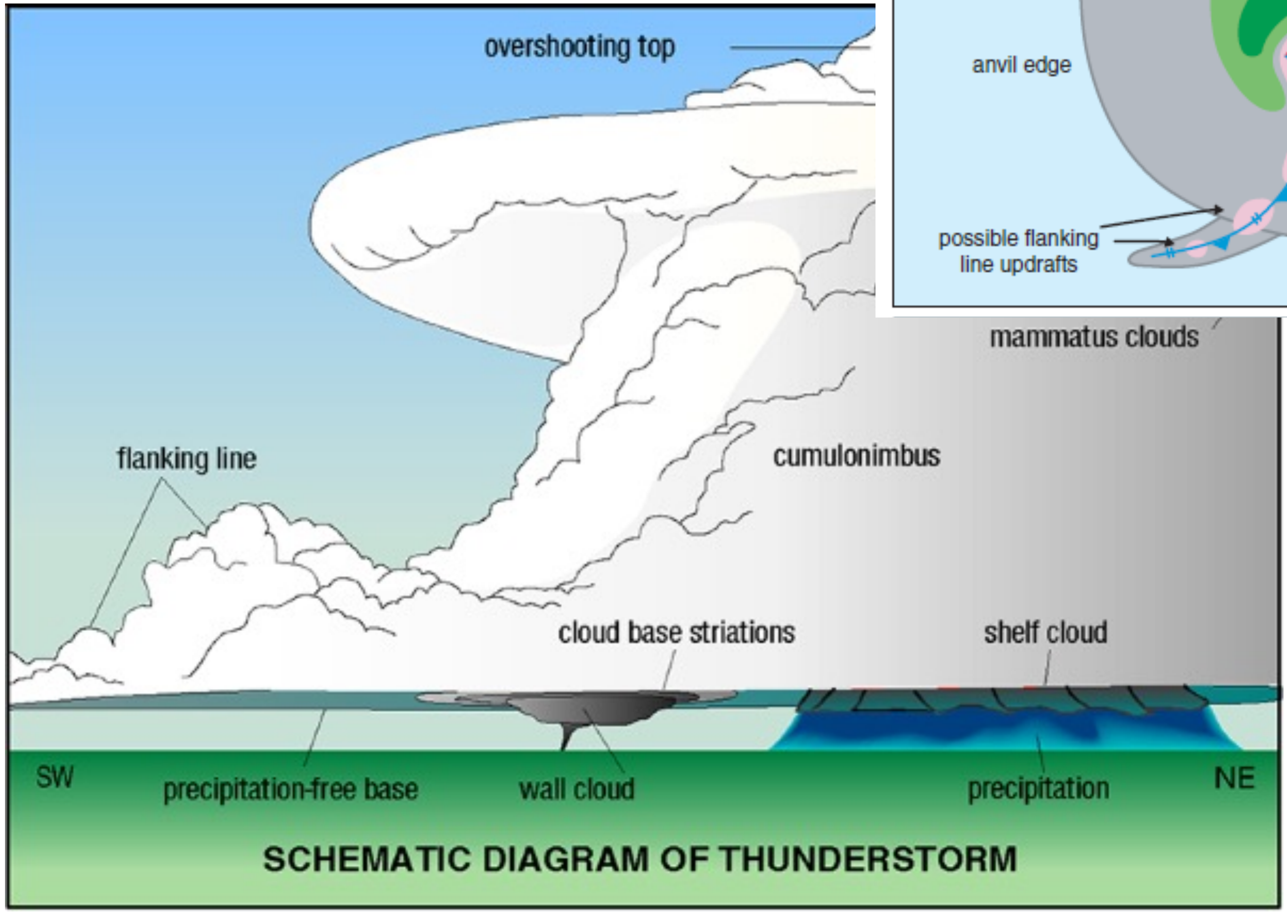

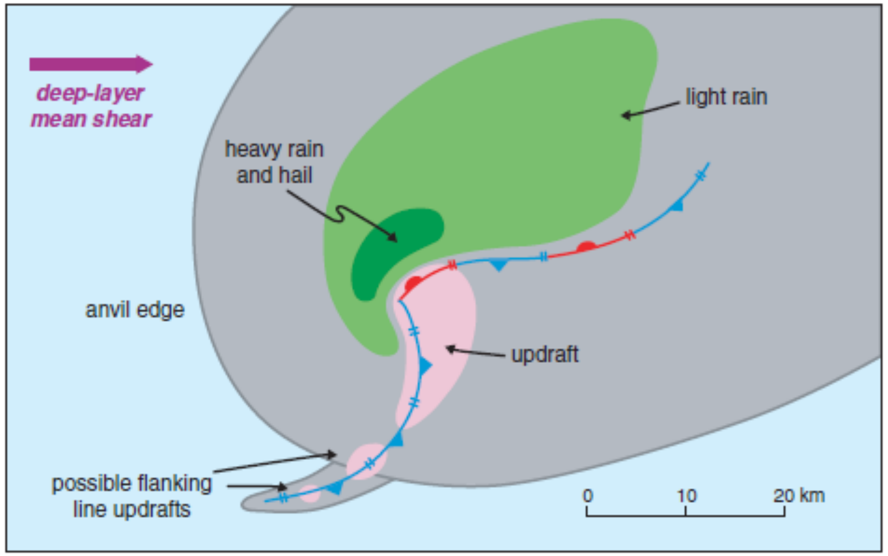

4） Downdraft

a. FFD: Forward-flank downdraft

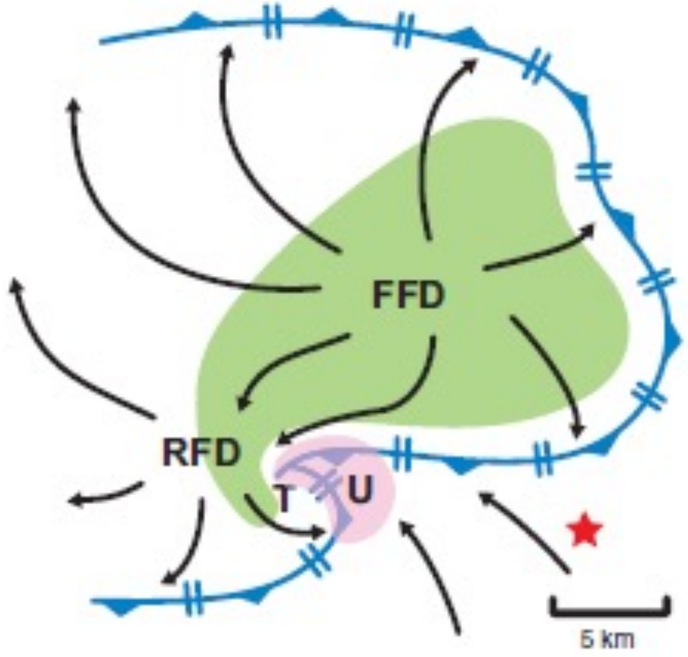

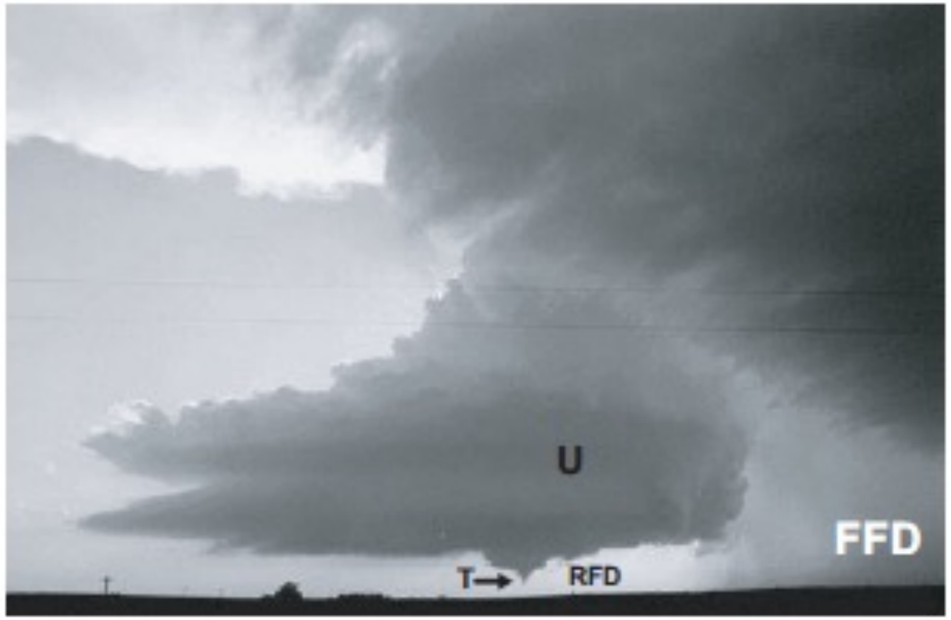

形成机制: 强的深厚垂直风切变，导致强的高层storm-relative wind， 致使降水粒子向前沉降。

指向下方的垂直气压梯度力。

4） Downdraft

b. RFD: Rear-flank downdraft, near hook echo

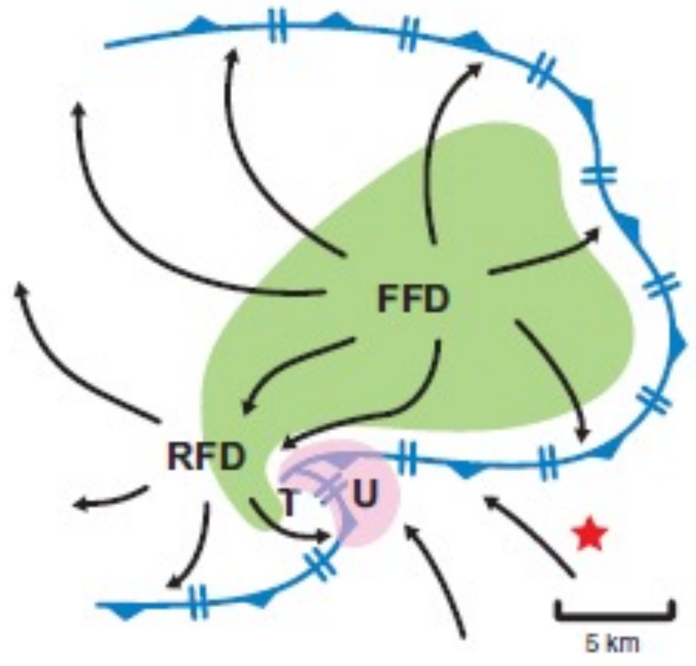

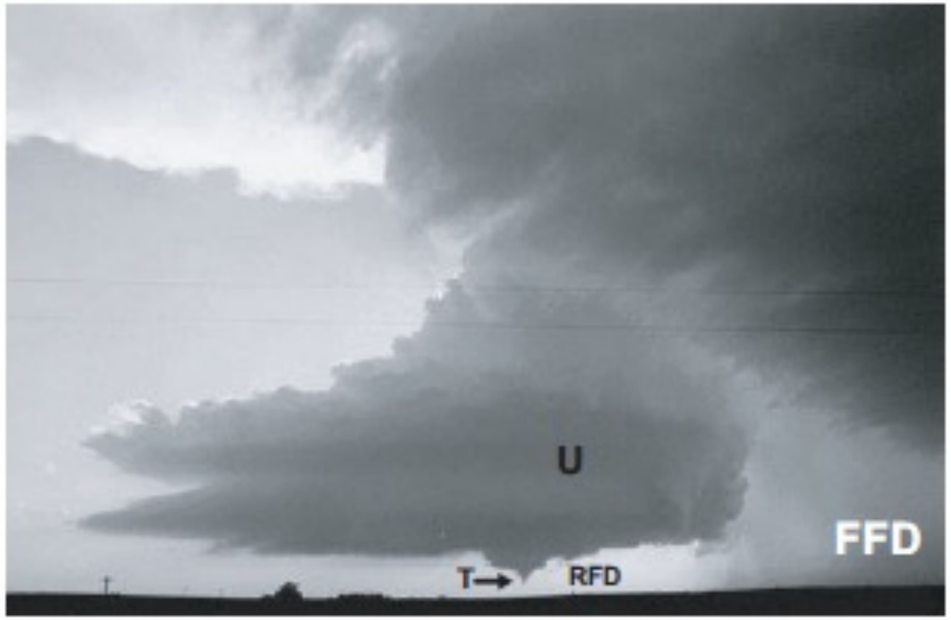

两个下沉支在地面形成类似于中纬度气旋锋面的阵风锋形状


mesocyclone
Forward flank
downdraft (FFD)
Rear flank
downdraft (RFD)
Weather-Photos.Net
© 2012 Marko Korošec

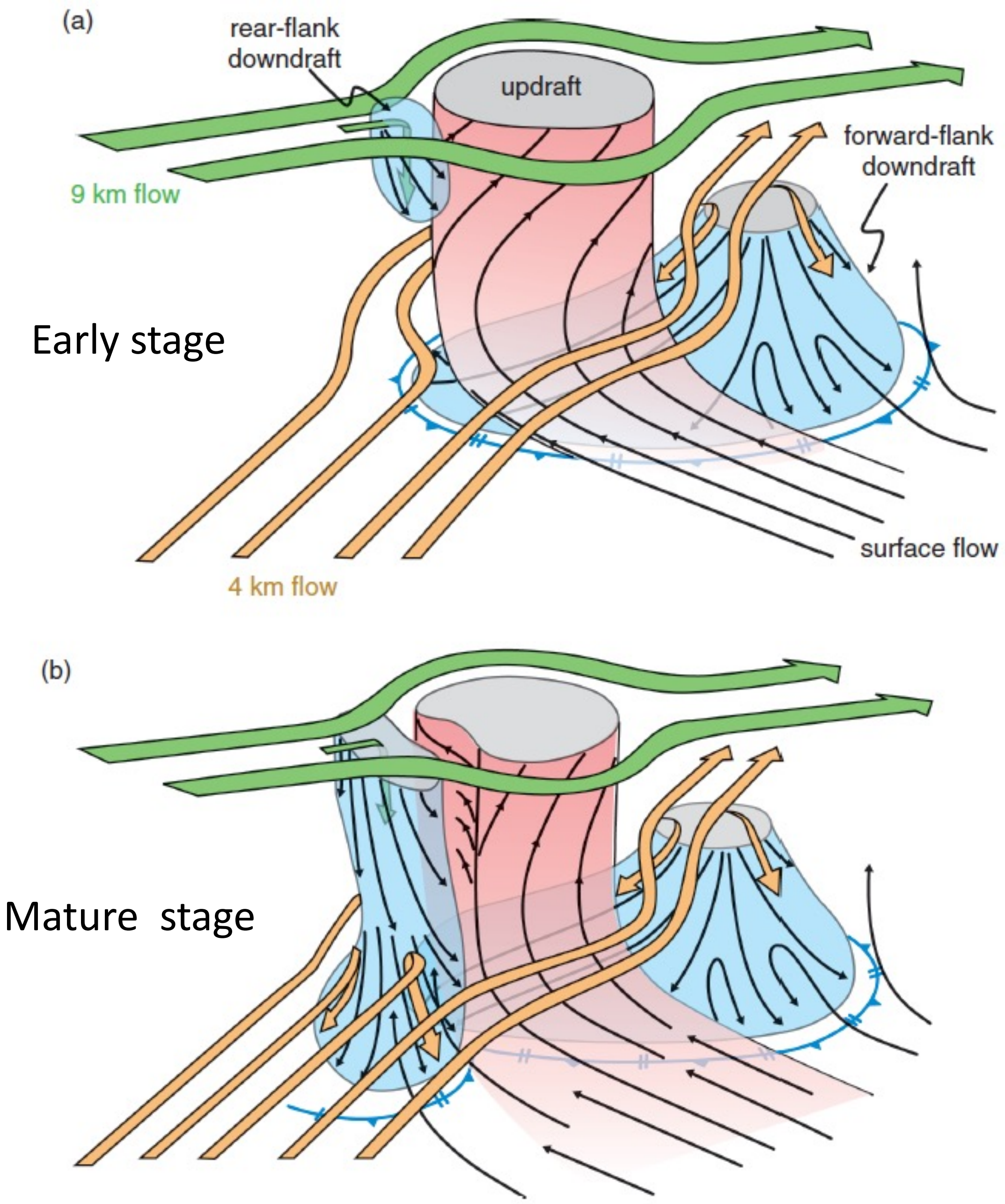

形成机制:

中上层干空气在上升气流后面导致蒸发冷却，产生负浮力（向下加速度）。

指向下方的垂直扰动气压梯度力。

5） Inflow lows

风速可能超过20m/s

最低气压为1–3 hPa

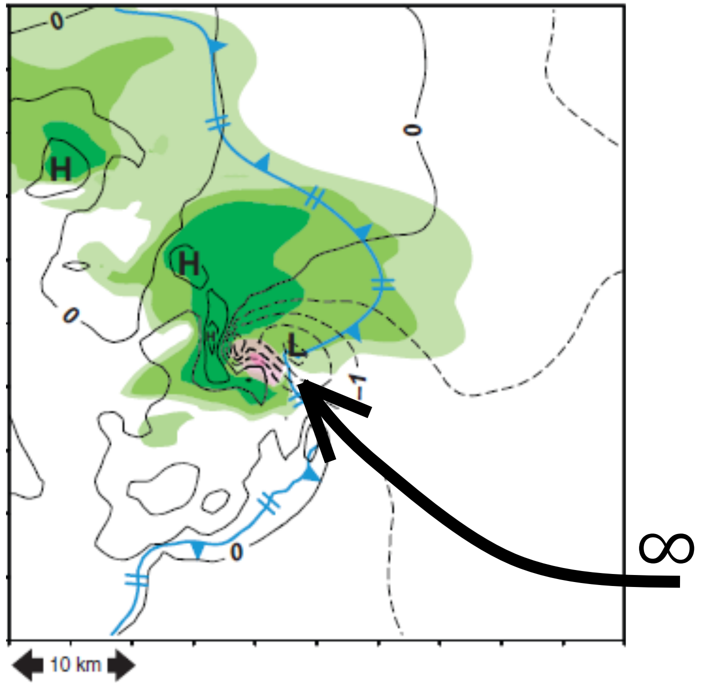

形成机制: 在刚体边界附近，表面气压扰动一般由Bernouli 方程表示

$$\frac{\rho v^2}{2} + p = Const$$

ρ, v, p分别为沿流线的空气密度、风速和气压。

风速大的地方气压低

$$\frac{\rho v_\infty^{\ 2}}{2} + p_\infty = \frac{\rho v^2}{2} + p \quad \Rightarrow \quad \Delta p = \frac{\rho (v^2 - v_\infty^{\ 2})}{2}$$

ρ=1 kg/m^3　v=20 m/s，　v_∞=5 m/s　$\Rightarrow$　$\Delta p = 2\ \text{hPa}$

6）降水分布

CL：classic supercell

LP：low-precipitation supercell

HP：high-precipitation supercell

CL：classic supercell

降水主要出现在前部

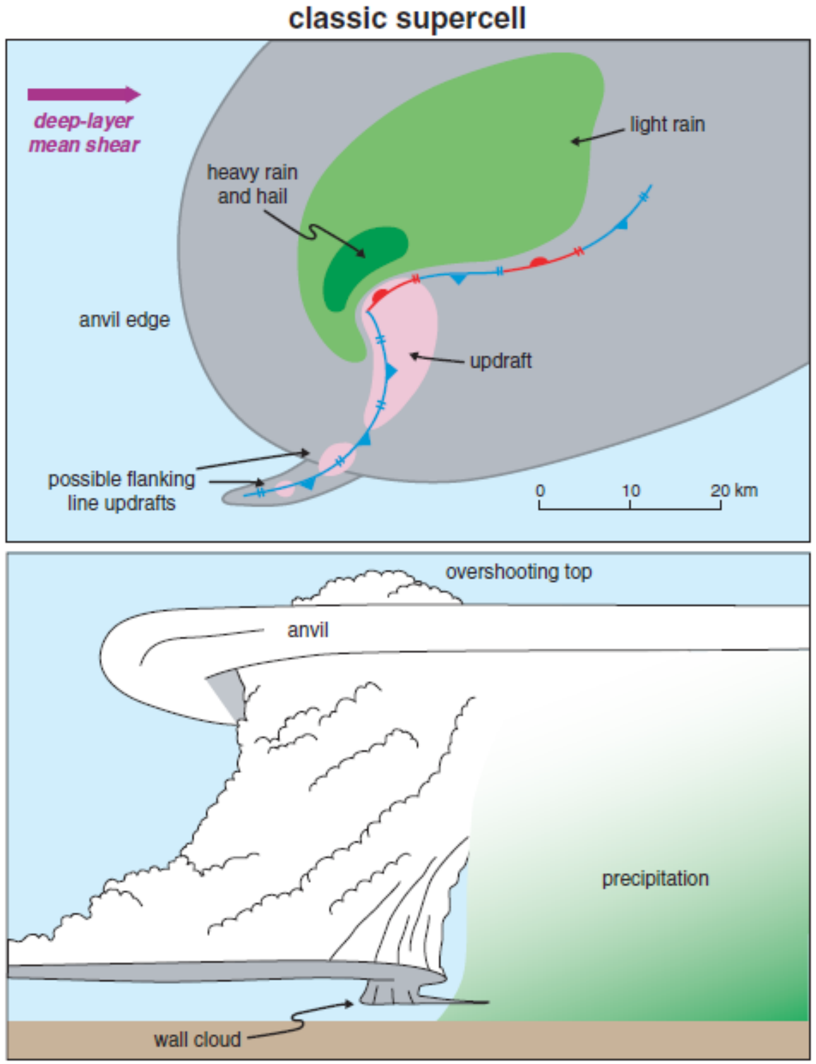

LP： low-precipitation supercell

降水完全与上升气流脱离，位于前部，大部分降水在下落中蒸发到不了地面。

雷达特征：Weak echo (< 45 dBZ), 无Hook echo，很少有龙卷。

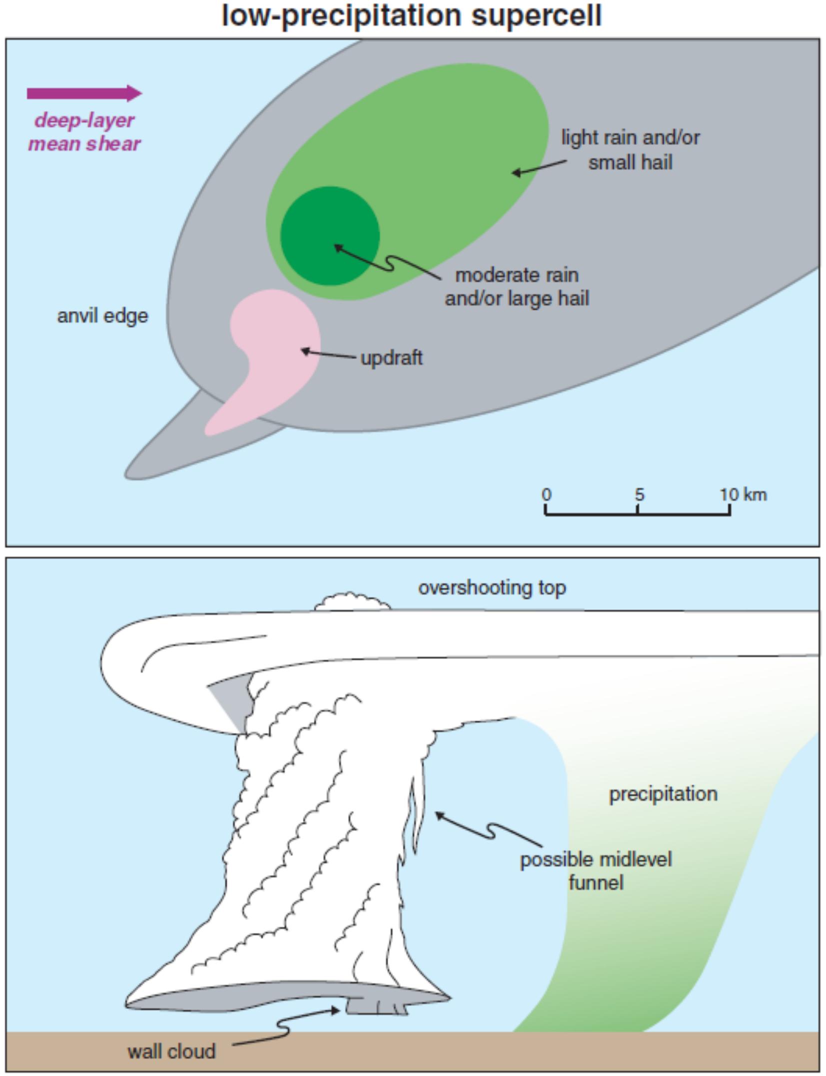

LP： low-precipitation supercell

HP：high-precipitation supercell

在Hook echo和后部有很大的降水，上升气流受降水遮挡很难看见。下沉气流很强。

雷达特征：云豆型。龙卷不如CL常见（下沉气流切断入流）。

天气：大冰雹，灾害性下击暴流。

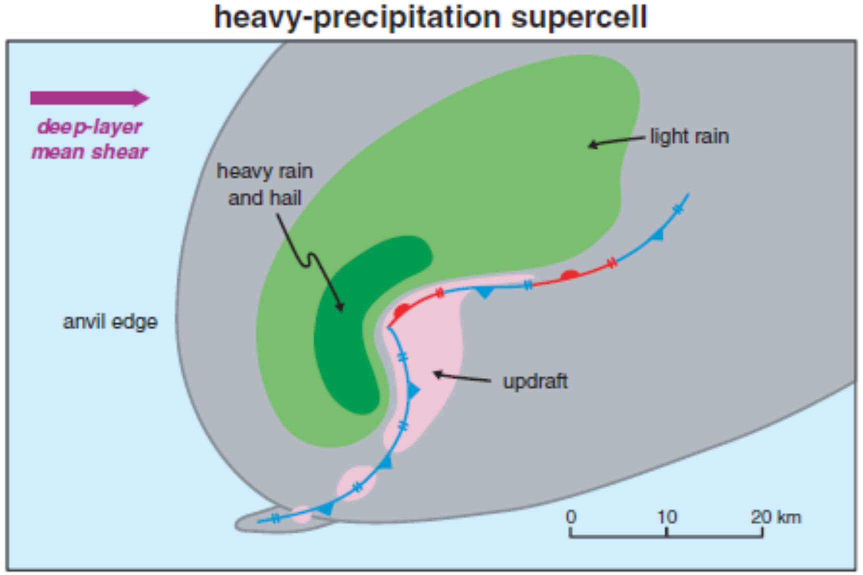

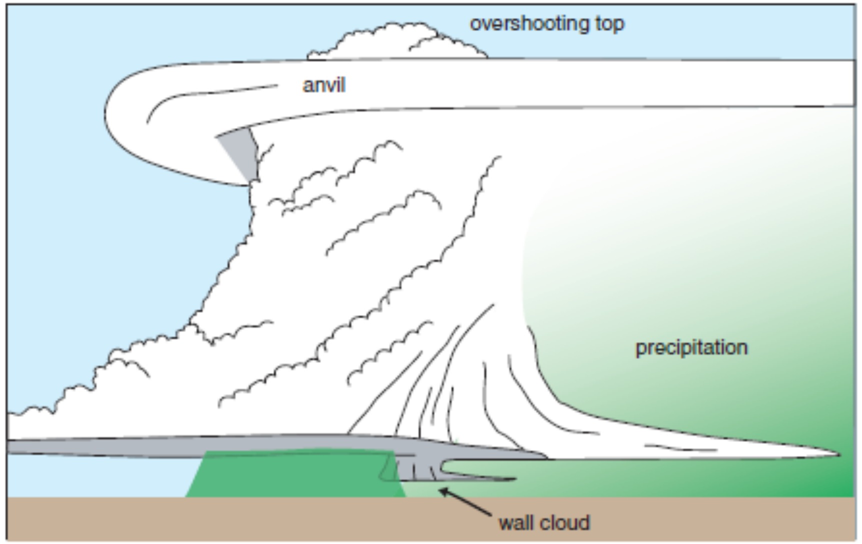

HP：high-precipitation supercell

7) mesocyclone

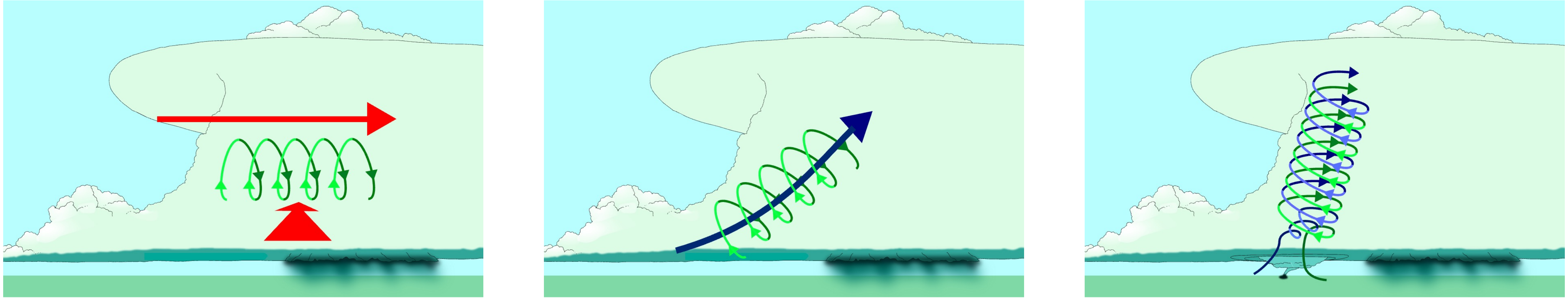

8) effects

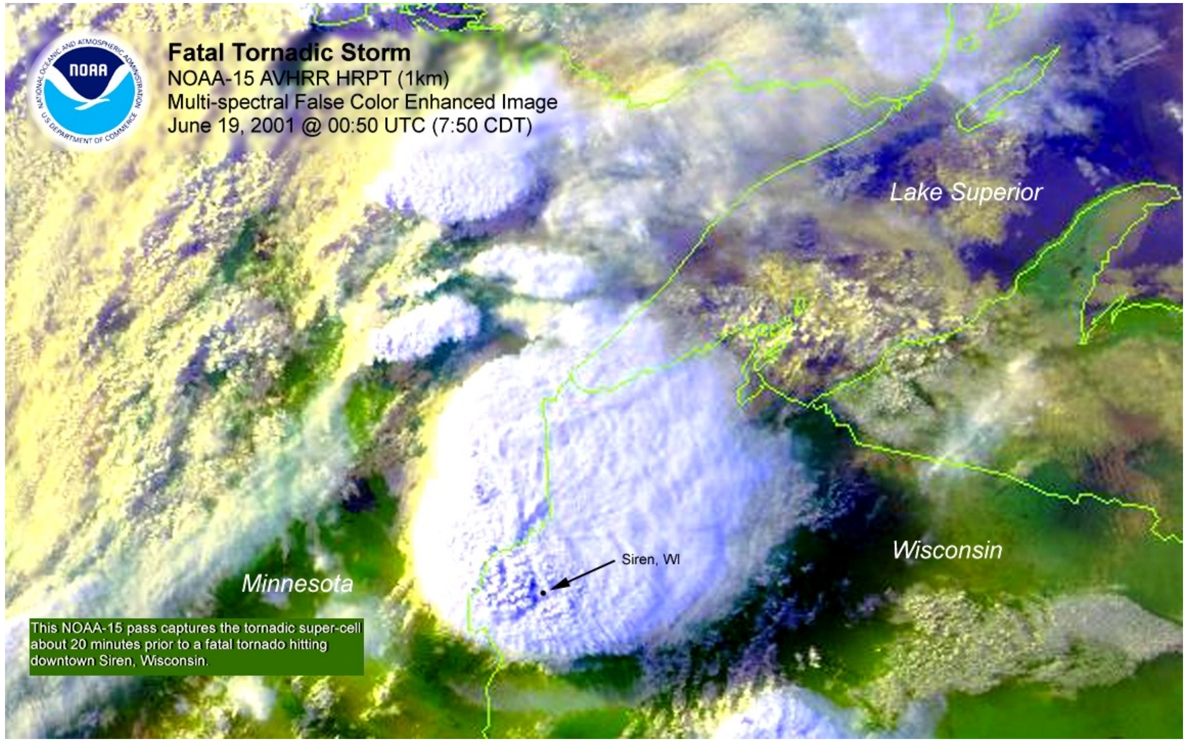

Supercells can produce hailstones averaging as large as two inches (5.1 cm) in diameter, winds over 70 miles per hour (110 km/h)[clarification needed], tornadoes of as strong as EF3 to EF5 intensity (if wind shear and atmospheric instability are able to support the development of stronger tornadoes), flooding, frequent-to-continuous lightning, and very heavy rain. Many tornado outbreaks come from clusters of supercells. Large supercells may spawn multiple long-tracked and deadly tornadoes, with notable examples in the 2011 Super Outbreak.

Severe events associated with a supercell almost always occur in the area of the updraft/downdraft interface. In the Northern Hemisphere, this is most often the rear flank (southwest side) of the precipitation area in **LP** and **classic** supercells, but sometimes the leading edge (southeast side) of **HP** supercells.

Note

a. 实际的风暴是连续变化的

b. LP， CL， HP与高层的storm-relative wind 密切相关。

HP < 18 m/s

18 m/s < CL < 28 m/s

28 m/s < LP

龙卷常发生在LP向CL的过度阶段。

c. 多雷暴并存时，临近雷暴的降水落入某雷暴可使之向HP转变。

Supplementary: Types of Clouds in the Earth's Atmosphere

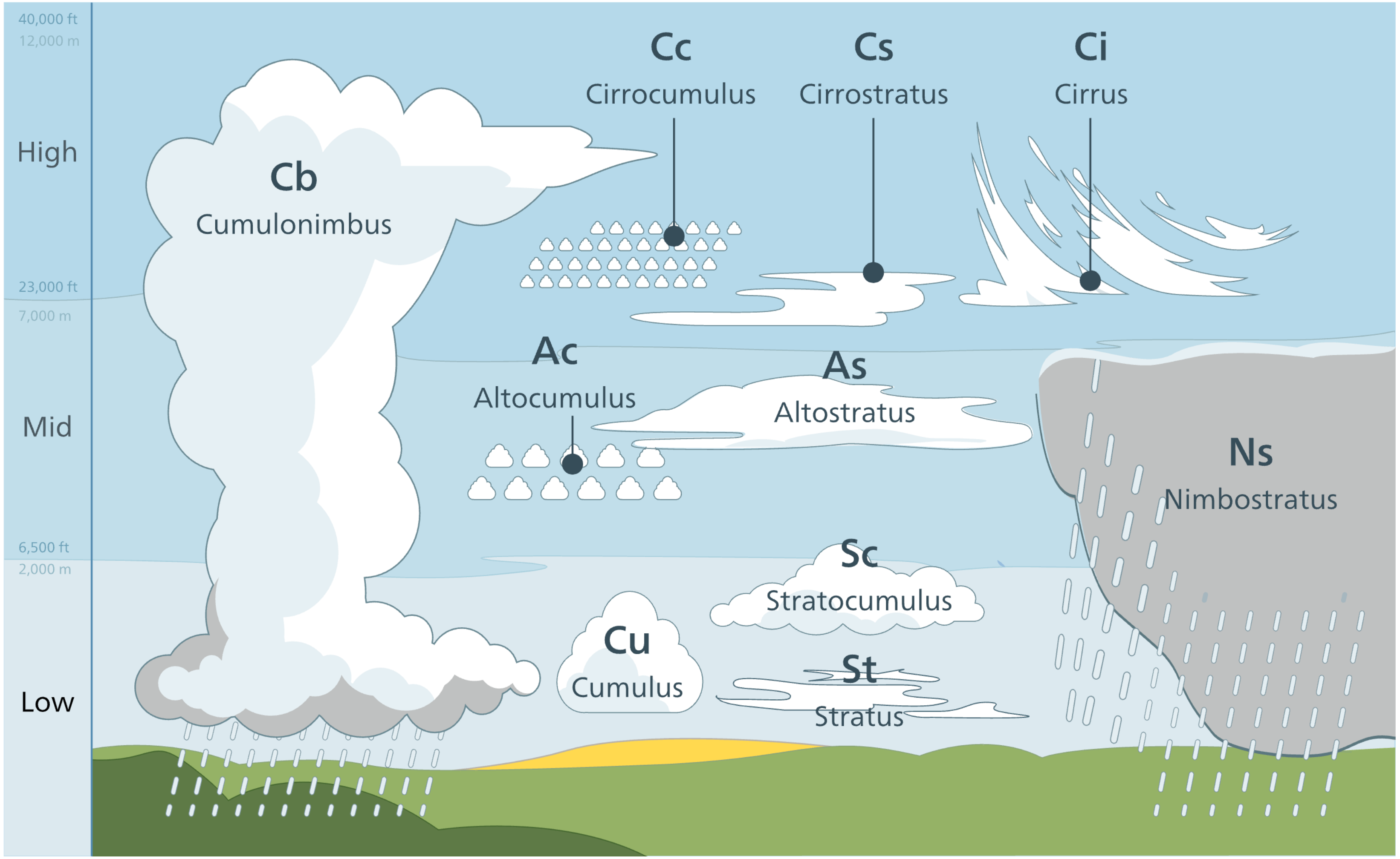

Genus	Étage
Cumulus	
Cumulonimbus	
Stratus	Low
Stratocumulus	
Nimbostratus	
Altostratus	Middle
Altocumulus	
Cirrus	
Cirrostratus	High
Cirrocumulus	

+ fog

Low Clouds: Cumulus

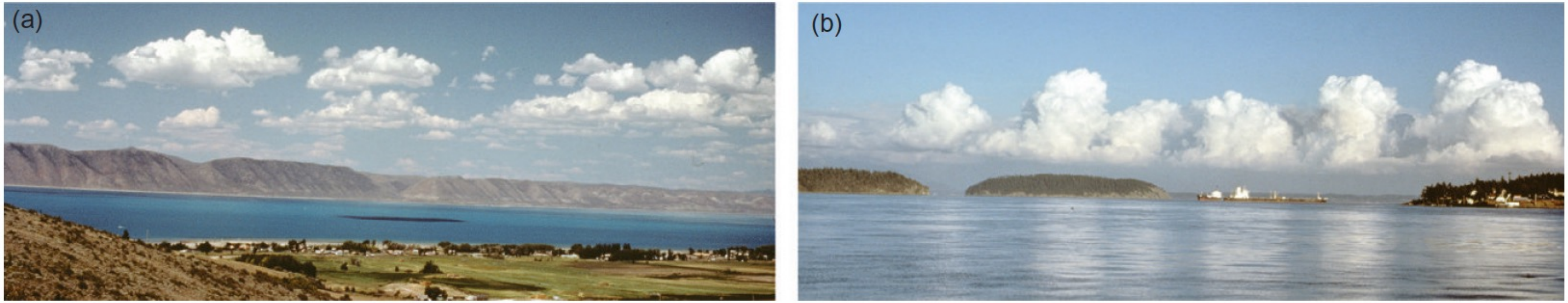

FIGURE 1.3 (a) Cumulus humilis. (b) Cumulus congestus over Puget Sound near Anacortes, Washington. *(a) Photo by Ronald L. Holle. (b) Photo by Steven Businger.*

non-precipitating

Low Clouds: Cumulonimbus

FIGURE 1.4 Time sequence showing cumulus congestus developing into cumulonimbus south of Key Biscayne, Florida. *Photos by Howard B. Bluestein.*

precipitating

Low Clouds: Cumulonimbus

FIGURE 1.5 Anvil of a cumulonimbus, as seen from Cimarron, Colorado. The anvil is classified as cirrus spissatus cumulonimbogenitus. If the anvil were more widespread, as from a line or group of cumulonimbus clouds, it would be classified as cirrostratus cumulonimbogenitus. *Photo by Ronald L. Holle*.

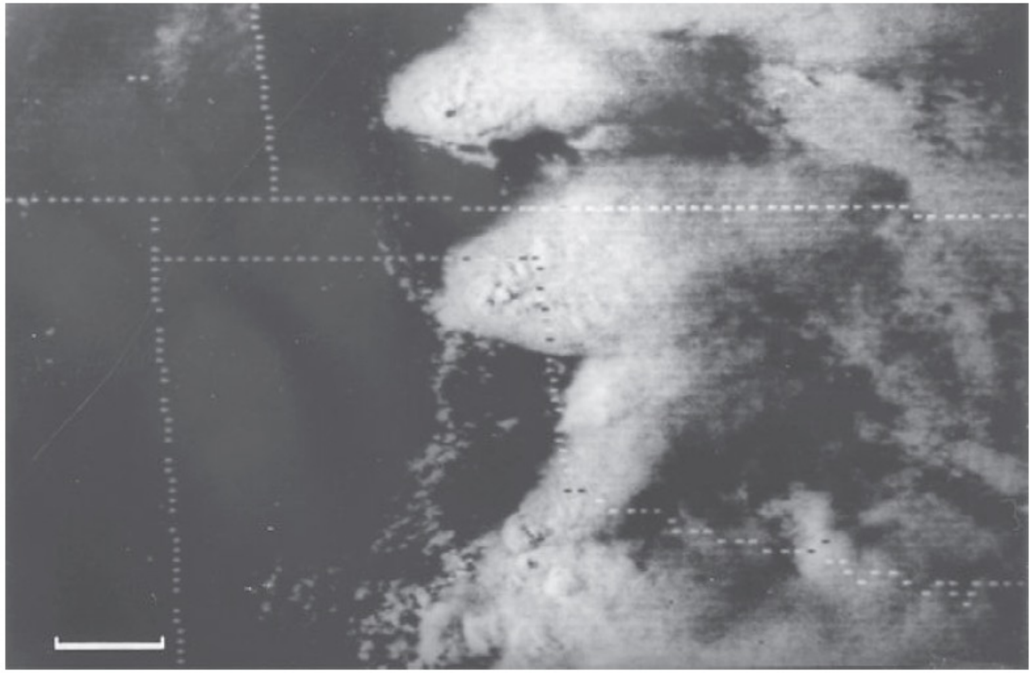

FIGURE 1.6 Visible wavelength satellite photograph of cumulonimbus anvils of supercell thunderstorms over Kansas, Oklahoma, and Texas. (Bar ~100 km.)

Low Clouds: Stratus

FIGURE 1.8 (a) Stratus cloud seen from the ground. (b) Stratus seen from Denny Mountain. Snoqualmie Pass, Washington. *(a) Photo by Reid Wolcott. (b) Photo by Steven Businger.*

Low Clouds: Stratocumulus

FIGURE 1.9 (a) Stratocumulus near Mitchell, South Dakota. (b) Stratocumulus seen from aircraft over the Atlantic Ocean, west of the southwest coast of England, toward north. *(a) Photo by Arthur L. Rangno. (b) Photo by Ronald L. Holle.*

Low Clouds: Stratocumulus

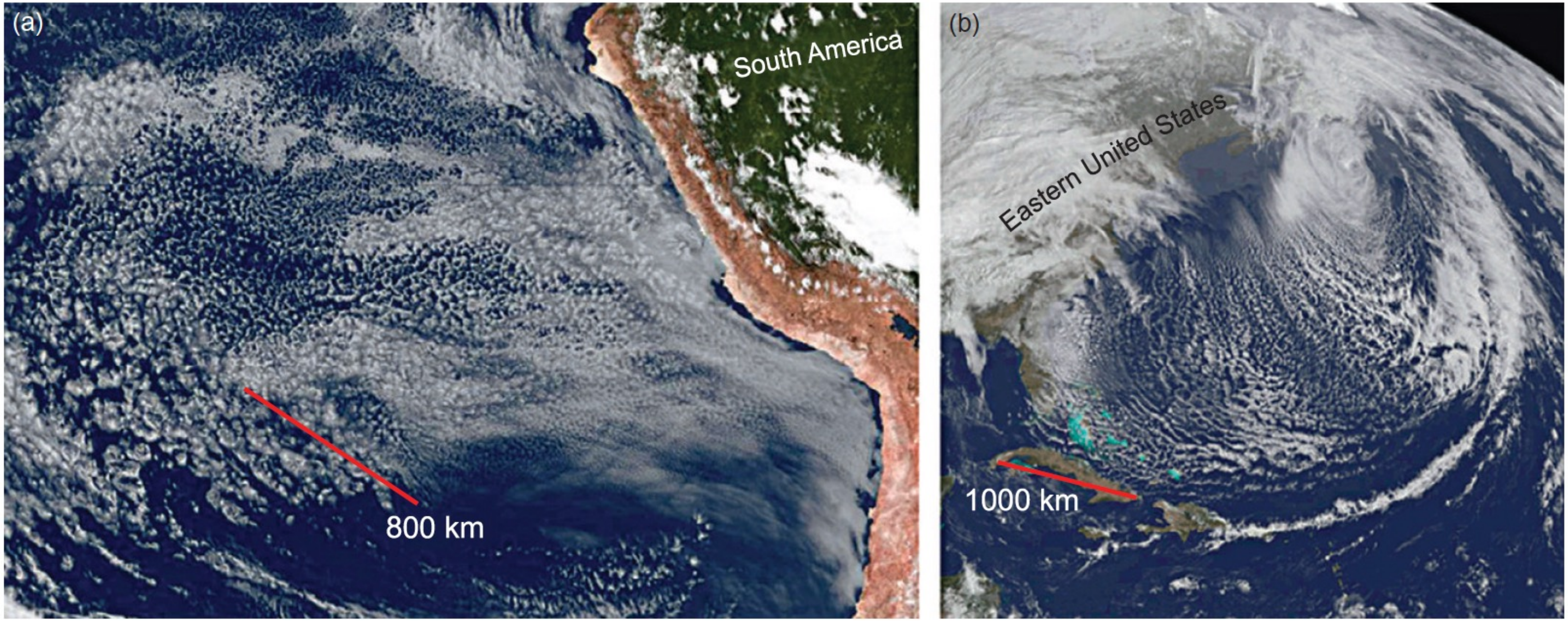

FIGURE 1.11 (a) Satellite view of stratocumulus off west coast of South America. (b) Satellite view of stratocumulus off the eastern and southeastern coast of North America. *NASA photos.*

Low Clouds: mixed clouds

FIGURE 1.10 "Cloud streets" viewed from aircraft. *Photo by Daniel Melconian, obtained with the photographer's permission via the Cloud Appreciation Society, with the aid of Gavin Pretor-Pinney and Ian Loxley.*

Low Clouds: Nimbostratus

FIGURE 1.12 Nimbostratus. From Guemes Island, looking toward Orcas Island, Puget Sound, Washington. *Photo by Steven Businger*.

Low Clouds: Fog

FIGURE 1.7 (a) Steam fog over a pond. (b) A shallow layer of radiation fog, sometimes called "ground fog." (c) Satellite view of fog in California's Central Valley. (d) Satellite view of advection fog and stratus cloud along the west coast of the United States. *(a) Free photo from cepolina.com. (b) Photo by Matthias Suessen. (c) NASA image, bar ~100 km. (d) NASA satellite photo, bar ~100 km.*

Middle Clouds: Altostratus

FIGURE 1.13 Altostratus. Bodø, Norway. *Photo by Steven Businger.*

Middle Clouds: Altocumulus

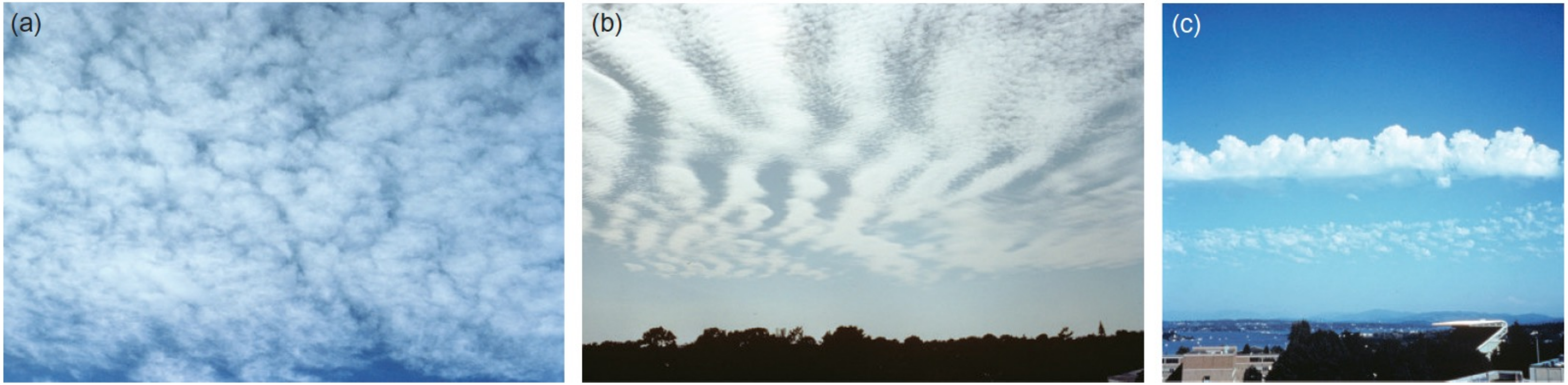

FIGURE 1.14 (a) Altocumulus stratiformis in the form of cellular clumps. (b) Altocumulus stratiformis in the form of long rolls (undulatus). (c) Altocumulus castellanus. Seattle, Washington. *(a, b) Photos by Ron Holle. (c) Photo by Arthur L. Rangno.*

High Clouds: Cirrus, Cirrostratus, Cirrocumulus

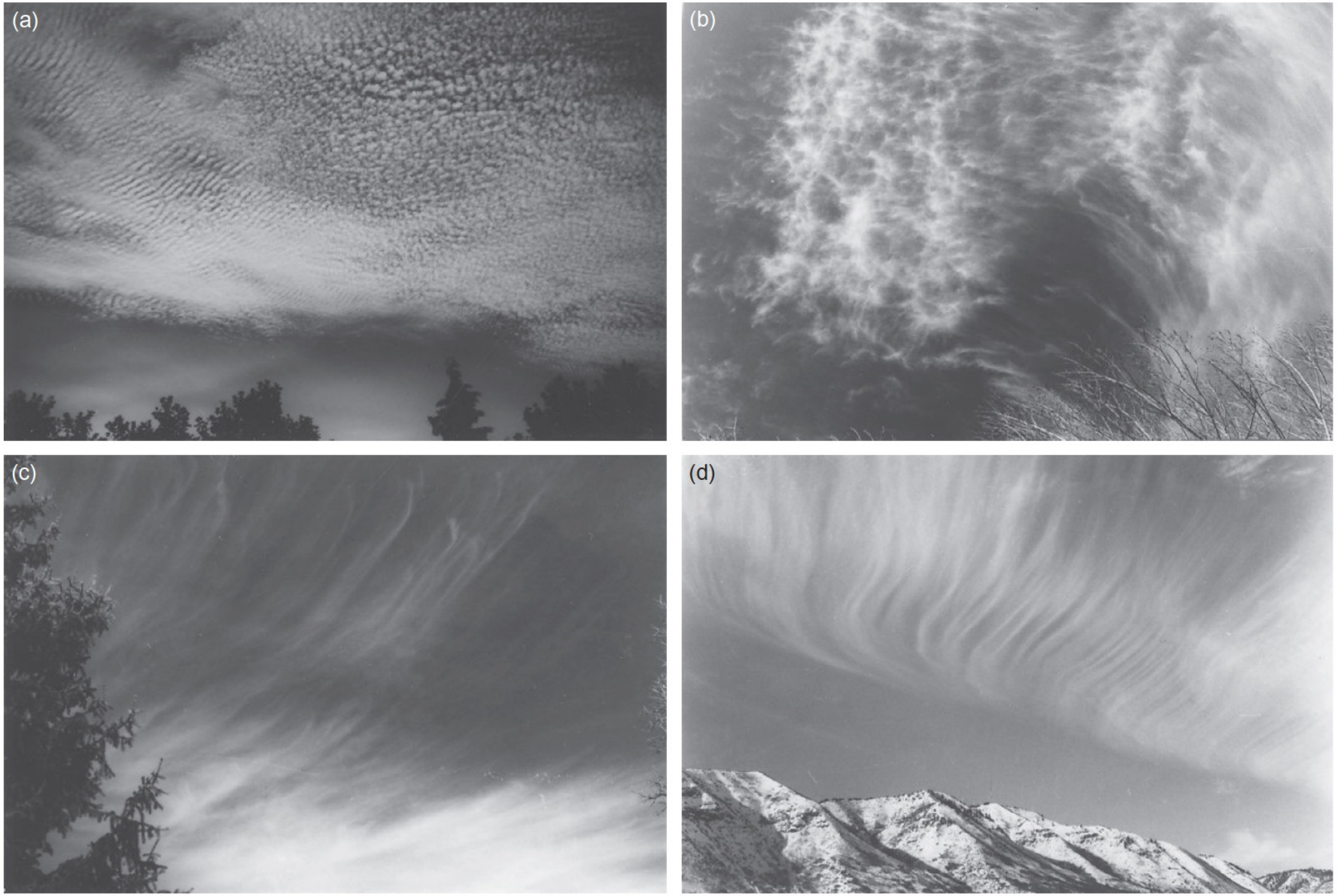

FIGURE 1.15 (a) Cirrocumulus stratiformis in the form of both undulatus and cells. Seattle, Washington. (b) Cirrus floccus. Durango, Colorado. (c) Cirrus uncinus. Durango, Colorado. (d) Cirrus fibratus vertebratus. Durango, Colorado. *Photos by Arthur L. Rangno.*

FIGURE 1.17 Cirrostratus with halo. *Photo by Reid Wolcott.*

Orographic Clouds

FIGURE 1.21 Looking upwind at a lenticular wave-cloud band (foreground) forming in the lee of the Continental Divide, which is far beyond the foot-hills seen in the foreground. Boulder, Colorado. *Photo by Dale R. Durran.*

FIGURE 1.22 Looking downwind at a series of lenticular wave clouds in the lee of the Continental Divide. Boulder, Colorado. *Photo by Dale R. Durran.*

FIGURE 1.20 Stacks of lenticular clouds in the lee of Mt. Rainier, in Washington State. Such clouds have sometimes been reported as UFOs. *Photo by Ian Bond.*

FIGURE 1.18 Cap cloud over Mount Rainier, Washington. *Photo by Ken Vensel.*

FIGURE 1.19 Horseshoe shaped cloud (Turusi) in lee of Mt. Fuji, Japan. *Photo taken in 1930 by Masanao Abe; see Abe (1932) for details.*

Orographic Clouds

FIGURE 1.23 Turbulent rotor cloud downwind (left-hand side of the photo) of the Sierra Nevada mountain range in the Owens Valley near Bishop. California. Downslope winds gather dust on the valley floor and serve as a tracer of the air rising suddenly up into the cloud. Over the mountains themselves (upper right of photo), a portion of the *Föhn* wall cloud is seen. *Photo courtesy of Morton G. Wurtele.*

FIGURE 1.24 *Föhn* wall cloud (right-hand side of photo) over the Dinaric Alps and turbulent rotor cloud (left-hand side of photo) downwind of the mountains. *Photo taken from an aircraft at about 6 km by Andreas Walker.*

FIGURE 1.25 *Föhn* wall cloud. Boulder, Colorado. *Photo by Dale R. Durran.*

FIGURE 1.26 Banner cloud on the Matterhorn, Switzerland. *Photo by Roger Colbeck.*

Noctilucent Clouds: 75-85km polar mesosphere

FIGURE 1.28 NASA Photo taken from the International Space Station. A thin layer of noctilucent cloud is seen in the mesosphere, which is well above where the sun below the horizon is shining through the troposphere from below the horizon. *NASA photo.*

FIGURE 1.29 Noctilucent cloud seen from the ground. *Photo by Martin Koitmäe.*

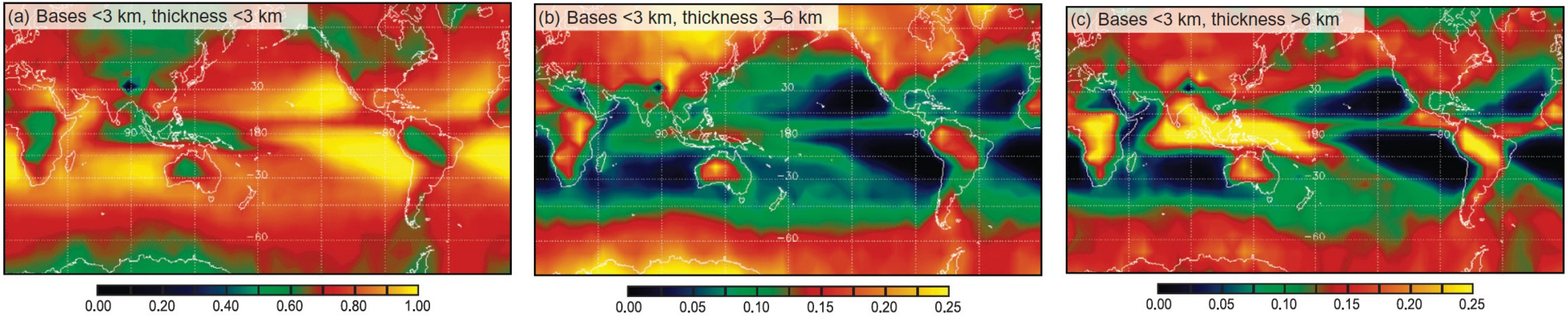

FIGURE 1.35 Coverage by clouds with low bases, as seen by CloudSat and CALIPSO satellites. (a) Stratus and stratocumulus frequency is indicated by fraction of low clouds observed at each grid point that have bases less than 3 km altitude and layer thicknesses less than 3 km. (b) Frequency of moderately deep clouds (most likely moderately deep convective or frontal clouds) seen at each grid point that have bases less than 3 km and layer thicknesses between 3 and 6 km. (c) Frequency of deep clouds (most likely deep convective or frontal clouds) seen at each grid point that have bases less than 3 km and layer thicknesses greater than 6 km. *The original versions of these figures appeared in Mace et al., 2009. They are republished here with permission of the American Geophysical Union. However, they have been updated with a larger, 4-year dataset and have been analyzed courtesy of Gerald Mace and Qiuqing Zhang at 5 km resolution instead of 80 km resolution.*

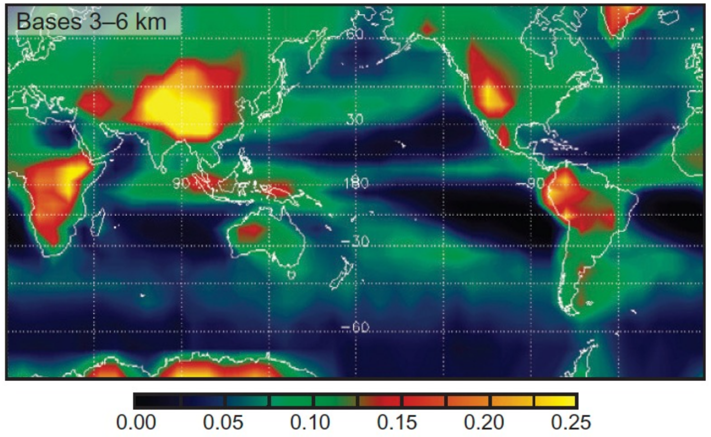

FIGURE 1.36 Coverage by clouds with bases greater than 6 km as seen by CloudSat and CALIPSO satellites. *The original version of this figure appeared in Mace et al., 2009. It is republished here with permission of the American Geophysical Union. However, the figure has been updated with a larger, 4-year, dataset and provided courtesy of Gerald Mace and Qiuqing Zhang. The new analysis is at 5 km resolution instead of 80 km resolution.*

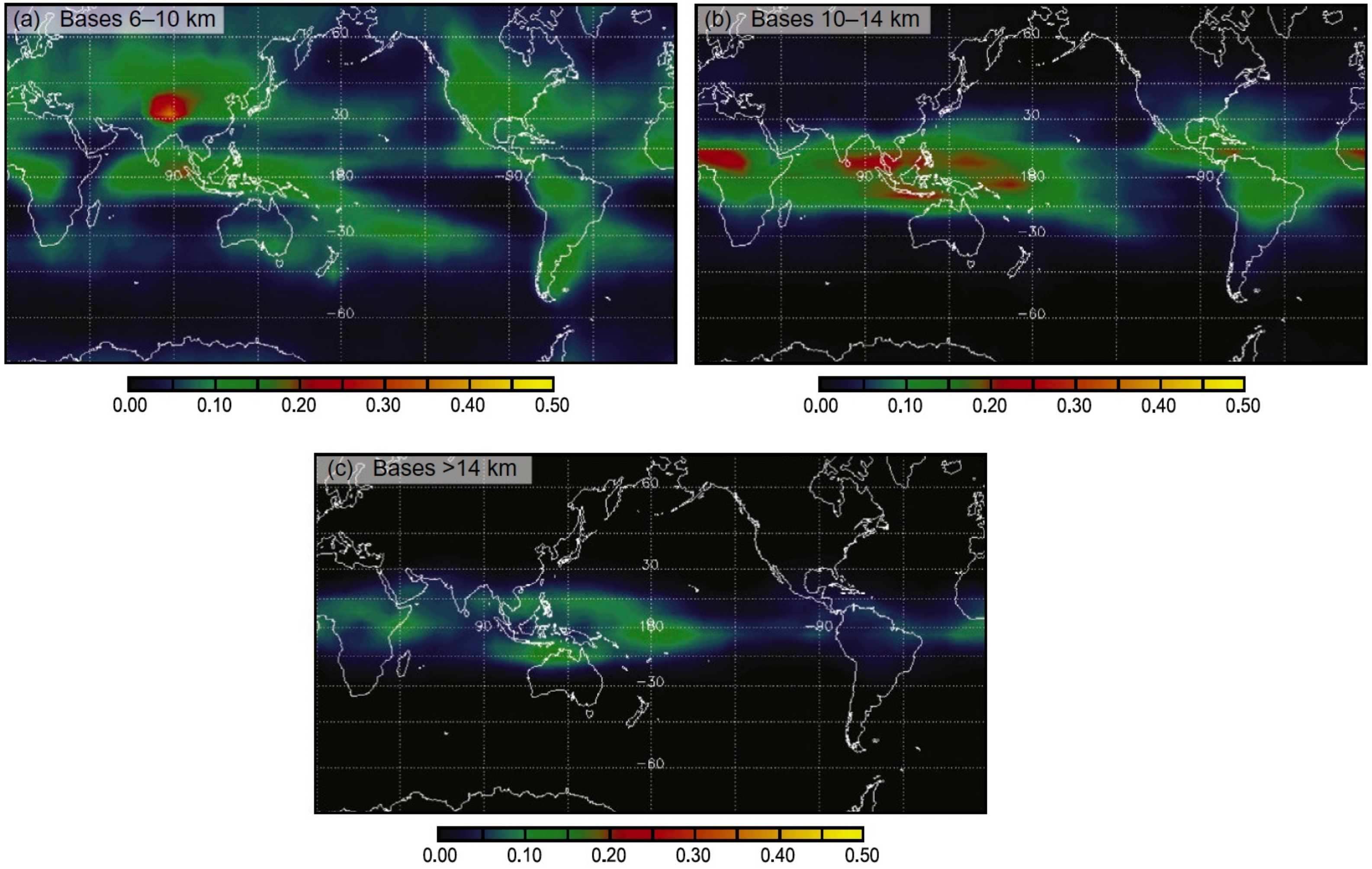

FIGURE 1.37 Coverage by clouds with bases between (a) 6–10 km, (b) 10–14 km, and (c) >14 km as seen by CloudSat and CALIPSO satellites. *The original version of this figure appeared in Mace et al., 2009. It is republished here with permission of the American Geophysical Union. However, the figure has been updated with a larger, 4-year dataset and provided courtesy of Gerald Mace and Qiuqing Zhang. The new analysis is at 5-km resolution instead of 80-km resolution.*